Inorganic Chemistry
Article

Inorg. Chem. **2010**, *49*, 2859–2871 **2859**
DOI: 10.1021/ic902399r

Hybrid Scorpionate/Cyclopentadienyl Magnesium and Zinc Complexes: Synthesis, Coordination Chemistry, and Ring-Opening Polymerization Studies on Cyclic Esters

Andrés Garcés,[†] Luis F. Sánchez-Barba,[*,†] Carlos Alonso-Moreno,[†,‡] Mariano Fajardo,[†] Juan Fernández-Baeza,[‡] Antonio Otero,[*,‡] Agustín Lara-Sánchez,[‡] Isabel López-Solera,[‡] and Ana María Rodríguez[‡]

[†]*Departamento de Química Inorgánica y Analítica, Universidad Rey Juan Carlos, Móstoles-28933-Madrid, Spain, and* [‡]*Departamento de Química Inorgánica, Orgánica y Bioquímica, Universidad de Castilla-La Mancha, Campus Universitario, 13071-Ciudad Real, Spain*

Received December 4, 2009

The reaction of the hybrid scorpionate/cyclopentadienyl lithium salt [Li(bpzcp)(THF)] [bpzcp = 2,2-bis(3,5-dimethylpyrazol-1-yl)-1,1-diphenylethylcyclopentadienyl] with 1 equiv of RMgCl proceeds cleanly to give very high yields of the corresponding monoalkyl κ^2-NN-η^5-C_5H_4 magnesium complexes [Mg(R)(κ^2-η^5-bpzcp)] (R = Me **1**, Et **2**, ^{n}Bu **3**, ^{t}Bu **4**, CH_2SiMe_3 **5**, CH_2Ph **6**). Hydrolysis of the hybrid lithium salt [Li(bpzcp)(THF)] with NH_4Cl/H_2O in ether cleanly affords the two previously described regioisomers: (bpzcpH) 1-[2,2-bis(3,5-dimethylpyrazol-1-yl)-1,1-diphenylethyl]-1,3-cyclopentadiene (**a**) and 2-[2,2-bis(3,5-dimethylpyrazol-1-yl)-1,1-diphenylethyl]-1,3-cyclopentadiene (**b**). Subsequent reaction of the bpzcpH hybrid ligand with ZnR_2 quantitatively yields the monoalkyl κ^2-NN-$\eta^1(\pi)$-C_5H_4 zinc complexes [Zn(R)-{κ^2-$\eta^1(\pi)$-bpzcp}] (R = Me **7**, Et **8**, ^{t}Bu **9**, CH_2SiMe_3 **10**). Additionally, magnesium alkyls **1**, **2**, **4**, and **5** can act as excellent cyclopentadienyl and alkyl transfers to the zinc metal center and yield zinc alkyls **7**−**10** in good yields. The single-crystal X-ray structures of the derivatives **4**, **5**, **7**, and **10** confirm a 4-coordinative structure with the metal center in a distorted tetrahedral geometry. Interestingly, whereas alkyl magnesium derivatives **4** and **5** present a η^5 coordination mode for the cyclopentadienyl fragment, zinc derivatives **7** and **10** feature a peripheral $\eta^1(\pi)$ arrangement in the solid state. Furthermore, the reaction of the hybrid lithium salt [Li(bpzcp)(THF)] with 1 equiv of $ZnCl_2$ in tetrahydrofuran (THF) affords very high yields of the chloride complex [ZnCl{κ^2-$\eta^1(\pi)$-bpzcp}] (**11**). Compound **11** was used as a convenient starting material for the synthesis of the aromatic amide zinc compound [Zn(NH-4-MeC_6H_4){κ^2-$\eta^1(\pi)$-bpzcp}] (**12**), by reaction with the corresponding aromatic primary amide lithium salt. Alternatively, aliphatic amide and alkoxide derivatives were only accessible by protonolysis of the bis(amide) complexes [M{$N(SiMe_3)_2$}$_2$] (M = Mg, Zn) and the mixed ligand complex [EtZnOAr)] with the hybrid ligand bpzcpH to afford [Zn(R){κ^2-$\eta^1(\pi)$-bpzcp}] (R = $N(SiMe_3)_2$ **13**, R = 2,4,6-$Me_3C_6H_2O$ **14**) and [Mg{$N(SiMe_3)_2$}(κ^2-η^5-bpzcp)] (**15**). Finally, alkyl and alkoxide-containing complexes **1**−**10** and **14** can act as highly effective single-component living initiators for the ring-opening polymerization of ε-caprolactone and lactides over a wide range of temperatures. ε-Caprolactone is polymerized within minutes to give high molecular weight polymers with medium-broad polydispersities ($M_n > 10^5$, $M_w/M_n = 1.45$). Lactide afforded poly(lactide) materials with medium molecular weights and polydispersities as narrow as $M_w/M_n = 1.02$. Additionally, polymerization of L-lactide occurred without racemization in the propagation process and offered highly crystalline, isotactic poly(L-lactides) with very high melting temperatures ($T_m = 165$ °C). Microstructural analysis of poly(*rac*-lactide) by ^{1}H NMR spectroscopy revealed that propagations occur without appreciable levels of stereoselectivity. Polymer end group analysis showed that the polymerization process is initiated by alkyl transfer to the monomer.

Introduction

In the present era of depleting fossil-based feedstocks and increasing environmental awareness, the exploration and improvement of new catalytic processes is crucial in the search for attractive alternatives to the bioresistant polyolefins.[1] Lactide, the cyclic dimer of lactic acid, is an inexpensive and annually renewable natural feedstock[2] that is a byproduct of biomass fermentation (e.g., beets and corn).

*To whom correspondence should be addressed. E-mail: luisfernando.sanchezbarba@urjc.es (L.F.S.-B.),antonio.otero@uclm.es (A.O.).

(1) (a) Allen, S. D.; Byrne, C. M.; Coates, G. W. *Feedstocks for the Future*; ACS Symposium Series 921; American Chemical Society: Washington, DC, 2006; Vol. *9*, pp 116−129. (b) Goodstein, D. *Out of Gas: The End of the Age of Oil*; W. W. Norton & Company: New York, 2004.

(2) (a) Coates, G. W.; Hillmyer, M. A. *Macromolecules* **2009**, *42*, 7987–7989. (b) Biela, T.; Kowalski, A.; Libiszowski, J.; Duda, A.; Penczek, S. *Macromol. Symp.* **2006**, 47–55.

Published on Web 02/10/2010

Ring-opening polymerization (ROP) of lactide[2a,3,4] yields poly(lactides) (PLAs), an important emerging bulk commodity material[5,6] given its utility in environmentally friendly and recyclable thermoplastics, which have the added benefit of biodegradability.[7,8] Additionally, the biocompatible nature[9] of lactide systems with living tissue and the nontoxicity of the bioassimilable PLAs has attracted significant attention in biomedical and pharmaceutical applications, for example, in resorbable surgical sutures,[9,10] drug delivery vehicles,[10] and artificial tissue matrixes.[11] These medicinal applications have promoted the use of biocompatible metals in the design of new catalysts, such as magnesium[12] and zinc[13,14] systems. Furthermore, zinc and magnesium-based catalysts have been extensively employed in ROP and are among the most efficient initiators used to date for the well-controlled polymerization of cyclic esters such as ε-caprolactone and lactides.[3,4,15−17]

In this context, our research group has recently reported amidinate-based heteroscorpionate ligands,[18] related to the bis(pyrazol-1-yl)methane system,[19] with different levels of steric congestion as convenient ancillary ligands for the synthesis of well-defined alkyl magnesium[20] and alkyl[21]-amide[22] zinc complexes of the type [M(R)(κ^3-NNN)] (M = Mg, Zn; R = alkyl, amide). Moreover, heteroscorpionate alkyl magnesium complexes proved to be highly effective single-component living initiators[20] for the well-controlled ROP of ε-caprolactone and lactides over a wide range of temperatures. Additionally, the more sterically hindered alkyl zinc initiators[21] offered good control of the polymer microstructures and promoted the formation of a heterotactic bias in the polymerization of *rac*-lactide. Furthermore, heteroscorpionate amide zinc[22] derivatives also behaved as efficient single-component initiators for the ROP of ε-caprolactone at room temperature.

The possibility of designing alternative magnesium and zinc initiators for efficient ROP stimulated our interest in a new scorpionate/cyclopentadienyl hybrid ligand of the type NNCp, derived from the bis(3,5-dimethylpyrazol-1-yl)-methane, to compare their synthetic accessibility, structural arrangements, and catalytic behavior in the ROP of these polar monomers with the previously reported amidinate-based magnesium[20] and zinc[21,22] analogues. This attractive scaffold, which was previously prepared in our group in the form of the lithium salt,[23,24b] has proven to act as an excellent ancillary ligand for the synthesis of discrete titanium[24] and zirconium[24] complexes and in efficient scandium and yttrium initiators for the ROP of cyclic esters[25a]

(3) (a) Platel, R. H.; Hodgson, L. M.; Williams, C. K. *Polym. Rev.* **2008**, *48*, 11–63. (b) Chisholm, M. H.; Zhou, Z. *J. Mater. Chem.* **2004**, *14*, 3081–3092. (c) Nakano, K.; Kosaka, N.; Hiyama, T.; Nozaki, K. *Dalton Trans.* **2003**, 4039–4050. (d) Coates, G. W. *J. Chem. Soc., Dalton Trans.* **2002**, 467–475. (e) O'Keefe, B. J.; Hillmyer, M. A.; Tolman, W. B. *J. Chem. Soc., Dalton Trans.* **2001**, 2215–2224.

(4) (a) Chisholm, M. H.; Zhou, Z. *Stereoselective Polymerization with Single Site Catalysts*; Baugh, L. S., Canich, J. A. M., Eds.; CRC Press: Boca Raton, FL, 2008; Chapter 25. (b) Wu, J.; Yu, T.-L.; Chen, C.-T.; Lin, C.-C. *Coord. Chem. Rev.* **2006**, *250*, 602–626. (c) Dechy-Cabaret, O. Martin-Vaca, B.; Bourissou, D. *Chem. Rev.* **2004**, *104*, 6147–6176.

(5) (a) Gruber, P. R.; O'Brien, M. *Biopolymers*; Steinbüchel, A., Doi, Y., Eds.; Wiley-VCH: Weinheim, Germany, 2002; Vol. *4*, pp 235−250. (b) Drumright, R. E.; Gruber, P. R.; Henton, D. E. *Adv. Mater.* **2000**, *12*, 1841–1846.

(6) (a) Vink, E. T. H.; Rábago, K. R.; Glassner, D. A.; Springs, B.; O'Connor, R. P.; Kolstad, J.; Gruber, P. R. *Macromol. Biosci.* **2004**, *4*, 551–564.

(7) (a) Coulembier, O.; Degée, P.; Hedrick, J. L.; Dubois, P. *Prog. Polym. Sci.* **2006**, *31*, 723–747. (b) Amgoune, A.; Thomas, C. M.; Roisnel, T.; Carpentier, J.-F. *Chem.—Eur. J.* **2006**, *12*, 169–179. (c) *Biopolymers*; Steinbüchel, A., Doi, Y., Eds.; Wiley-VCH: Weinheim, Germany, 2002; Vol. *4*. (d) Ikada, Y.; Tsuji, H. *Macromol. Rapid Commun.* **2000**, *21*, 117–132. (e) Chiellini, E.; Solaro, R. *Adv. Mater.* **1996**, *8*, 1375–1381.

(8) (a) Vink, E. T. H.; Rábago, K. R.; Glassner, D. A.; Gruber, P. R. *Polym. Degrad. Stab.* **2003**, *80*, 403–419. (b) http://www.natureworksllc.com/.

(9) (a) Williams, S. F.; Martin, D. P. *Biopolymers*; Steinbüchel, A., Doi, Y., Eds.; Wiley-VCH: Weinheim, Germany, 2002; Vol. *4*, pp 91−127. (b) Frazza, E. J.; Schmitt, E. E. J. *Biomed. Mater. Res. Symp.* **1971**, *1*, 43–58. (c) Schmitt, E. E.; Polistina, R. A. U.S. Patent 3, 463, 158, **1969**. (d) Dexon and Vicryl are products of Davis & Geek Corp., Wayne, NJ, and Ethicon Inc., Somerville, NJ, respectively.

(10) (a) Jerome, C.; Lecomte, P. *Adv. Drug Delivery Rev.* **2008**, *60*, 1056–1076. (b) Penczek, S.; Cypryk, M.; Duda, A.; Kubisa, P.; Slomkowski, S. *Prog. Polym. Sci.* **2007**, *32*, 247–282. (c) Bourissou, D.; Moebs-Sanchez, S.; Martin-Vaca, B. *C. R. Chim.* **2007**, *10*, 775–794. (d) Leupron Depot is a product of Takeda Chemical Industries, Ltd., Japan, for drug delivery purposes. (e) Taehan Hwakakhoe Chi 34, 203; *Chem. Abstr.* **1990**, *113*, 98014g.

(11) (a) Chisholm, M. H.; Iyer, S. S.; McCollum, D. G.; Pagel, M.; Werner-Zwanziger, U. *Macromolecules* **1999**, *32*, 963–973. (b) Hubbell, J. A.; Langer, R. *Chem. Eng. News* **1995**, *Mar 13*, 42–54. (c) Langer, R.; Vacanti, J. P. *Science* **1993**, *260*, 920–926.

(12) (a) *The Biological Chemistry of Magnesium*; Cowan, J. A., Ed.; VCH: New York, 1995. (b) Campbell, N. A. *Biology*, 3rd ed.; Benjamin/Cummings Publishing Company: Redwood City, CA, 1993; pp 718 and 811.

(13) Parkin, G. *Chem. Commun.* **2000**, 1971–1985.

(14) Mills, C. F. *Zinc in Human Biology*; Springer-Verlag: New York, 1989.

(15) (a) Wheaton, C. A.; Hayes, P. G.; Ireland, B. J. *Dalton Trans.* **2009**, 4832–4846. (b) Helou, M.; Miserque, O.; Brusson, J.-M.; Carpentier, J.-F.; Guillaume, S. M. *Adv. Synth. Catal.* **2009**, *351*, 1312–1324. (c) Labourdette, G.; Lee, D. J.; Patrick, O.; Ezhova, M. B.; Mehrkhodavandi, P. *Organometallics* **2009**, *28*, 1309–1319. (d) Chen, M.-T.; Chang, P.-J.; Huang, C.-A.; Peng, K.-F.; Chen, C.-T. *Dalton Trans.* **2009**, 9068–9074. (e) Helou, M.; Miserque, O.; Brusson, J.-M.; Carpentier, J.-F.; Guillaume, S. M. *Chem.—Eur. J.* **2008**, *14*, 8772–8775. (f) Marshall, E. L.; Gibson, V. C.; Rzepa, H. S. *J. Am. Chem. Soc.* **2005**, *127*, 6048–6051.

(16) (a) Allen, S.; Coates, G. W.; Jeske, R. Patent Number(s): WO2009025850-A2; WO2009025850-A3; WO2009025850-A4. Cornell Res. Found Inc. (b) Jeske, R. C.; DiCiccio, A. M.; Coates, G. W. *J. Am. Chem. Soc.* **2007**, *129*, 11330–11331. (c) Chamberlain, B. M.; Cheng, M.; Moore, D. R.; Ovitt, E. B.; Lobkovsky, E. B.; Coates, G. W. *J. Am. Chem. Soc.* **2001**, *123*, 3229–3238. (d) Chen, M.; Attygalle, A. B.; Lobkovsky, E. B.; Coates, G. W. *J. Am. Chem. Soc.* **1999**, *121*, 11583–11584.

(17) (a) Chisholm, M. H.; Gallucci, J. C.; Yaman, G. *Dalton Trans.* **2009**, 368–374. (b) Chisholm, M. H.; Galluci, J.; Phomphrai, K. *Chem. Commun.* **2003**, 48–49. (c) Chisholm, M. H.; Galluci, J.; Phomphrai, K. *Inorg. Chem.* **2002**, *41*, 2785–2794. (d) Chisholm, M. H.; Eilerts, N. W.; Huffman, J. C.; Iyer, S. S.; Pacold, V.; Phomphrai, K. *J. Am. Chem. Soc.* **2000**, *122*, 11845–11854. (e) Chisholm, M. H.; Eilerts, N. W. *Chem. Commun.* **1996**, 853–854.

(18) Otero, A.; Fernández-Baeza, J.; Antiñolo, A.; Tejeda, J.; Lara-Sánchez, A.; Sánchez-Barba, L. F; López-Solera, I.; Rodríguez, A. M. *Inorg. Chem.* **2007**, *46*, 1760–1770.

(19) (a) Otero, A.; Fernández-Baeza, J.; Lara-Sánchez, A.; Tejeda, J.; Sánchez-Barba, L. F. *Eur. J. Inorg. Chem.* **2008**, 5309–5326. (b) Pettinari, C.; Pettinari, R. *Coord. Chem. Rev.* **2005**, *249*, 663–691. (c) Bigmore, H. R.; Lawrence, S. C.; Mountford, P.; Tredget, C. S. *Dalton Trans.* **2005**, 635–651. (d) Otero, A.; Fernández-Baeza, J.; Antiñolo, A.; Tejeda, J.; Lara-Sánchez, A. *Dalton Trans.* **2004**, 1499–1510.

(20) Sánchez-Barba, L. F.; Garcés, A.; Fajardo, M.; Alonso-Moreno, C.; Fernández-Baeza, J.; Otero, A.; Antiñolo, A.; Tejeda, J.; Lara-Sánchez, A.; López-Solera, M. I. *Organometallics* **2007**, *26*, 6403–6411.

(21) Alonso-Moreno, C.; Garcés, A.; Sánchez-Barba, L. F.; Fajardo, M.; Fernández-Baeza, J.; Otero, A.; Antiñolo, A.; Lara-Sánchez, A.; Broomfield, L.; López-Solera, I.; Rodríguez, A. M. *Organometallics* **2008**, *27*, 1310–1321.

(22) Sánchez-Barba, L. F.; Alonso-Moreno, C.; Garcés, A.; Fajardo, M.; Fernández-Baeza, J.; Otero, A.; Lara-Sánchez, A.; Rodríguez, A. M.; López-Solera, I. *Dalton. Trans.* **2009**, 8054–8062.

(23) Otero, A.; Fernández-Baeza, J.; Antiñolo, A.; Tejeda, J.; Lara-Sánchez, A.; Sánchez-Barba, L.; Rodríguez, A. M.; Maestro, M. A. *J. Am. Chem. Soc.* **2004**, *126*, 1330–1331.

(24) (a) Otero, A.; Fernández-Baeza, J.; Antiñolo, A.; Tejeda, J.; Lara-Sánchez, A.; Sánchez-Barba, L. F.; Sánchez-Molina, M.; Rodríguez, A. M.; Bo, C.; Urbano-Cuadrado, M. *Inorg. Chem. Acta* **2009**, *362*, 2909–2914. (b) Otero, A.; Fernández-Baeza, J.; Antiñolo, A.; Tejeda, J.; Lara-Sánchez, A.; Sánchez-Barba, L. F.; Sánchez-Molina, M.; Rodríguez, A. M; Bo, C.; Urbano-Cuadrado, M. *Organometallics* **2007**, *26*, 4310–4320.

Chart 1. Possible Coordination Modes of the Cyclopentadienyl Ligand in Metallocenes

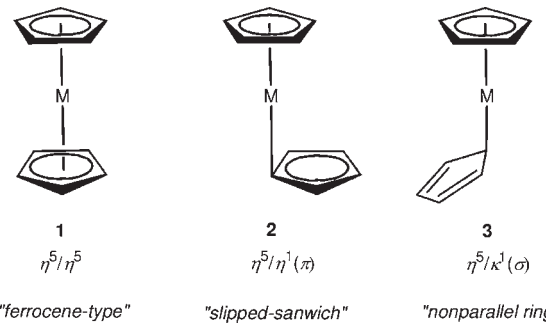

and styrene polymerization.[25b] Related cyclopentadienyl/scorpionate hybrid ligands derived from hydrobis(3,5-dimethylpyrazolyl)borate have been also reported.[26]

In the field of cyclopentadienyl-containing metal complexes it is usual to find different metal-cyclopentadienyl coordination modes. Thus, the most representative example, a η^5 coordination mode for the cyclopentadienyl fragment, appears in metallocenes, which exhibit a *ferrocene-type* structure (**1**), and in bent-metallocenes. Furthermore, cyclopentadienyl derivatives of the main-group elements present a rich variety of coordination modes, including a $\eta^1(\pi)$ coordination one which involves metal coordination through one sp^2-hybridized carbon atom of the ring by means of the π cloud. This is found in the complexes exhibiting $\eta^5/\eta^1(\pi)$ *slipped-sandwich* geometries (**2**). Additionally, it is possible to find a rigid $\kappa^1(\sigma)$ −Cp coordination mode with two localized C═C double bonds in the ring, giving rise to $\eta^5/\kappa^1(\sigma)$ complexes where the two cyclopentadienyl rings are not parallel (**3**) (Chart 1).[27] In particular, cyclopentadienyl derivatives of magnesium and zinc may adopt a variety of structures. For instance, whereas magnesium complexes predominately present a η^5-cyclopentadienyl coordination mode,[28a−c] with the exception of very few cases,[28d] interestingly, zinc derivatives offer a rich structural diversity in the hapticity count from η^1 or κ^1 to η^5, as recently reported by Carmona et al.[27a] in zincocenes with substituted cyclopentadienyl rings.

The work described here concerns a new approach in the chemistry of these biocompatible metals and, from this viewpoint, our initial study was aimed at preparing novel organomagnesium and zinc complexes of the type [M(R)(NNCp)].

Scheme 1. Synthesis of Scorpionate/Cyclopentadienyl Magnesium Alkyls [Mg(R)(κ^2-η^5-bpzcp)] (**1**−**6**)

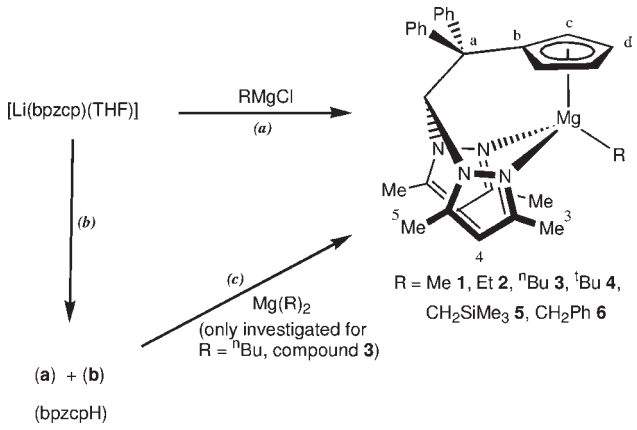

The study of the different structural arrangements for the two metals, their reactivity against nucleophilic reagents, and the use of these materials as single-component living initiators for the ROP of ε-caprolactone and L-/*rac*-lactide under well-controlled conditions are also discussed in detail.

Results and Discussion

Synthesis and Characterization of Scorpionate/Cyclopentadienyl Monoalkyl Magnesium and Zinc Complexes. A toluene solution of the hybrid scorpionate/cyclopentadienyl lithium salt [Li(bpzcp)(THF)][23,24b] [bpzcp = 2,2-bis(3,5-dimethylpyrazol-1-yl)-1,1-diphenylethylcyclopentadienyl] was treated with a series of commercially available Grignard reagents RMgCl in Et_2O or *n*-hexane solutions in a 1:1 molar ratio at −70 °C. These reactions gave the corresponding alkyl magnesium complexes [Mg(R)(κ^2-η^5-bpzcp)] (R = Me **1**, Et **2**, ^{t}Bu **4**, CH_2SiMe_3 **5**, CH_2Ph **6**) as yellow or orange solids in good yields (ca. 80%) after the appropriate workup (see Scheme 1a). Furthermore, hydrolysis of the aforementioned hybrid lithium salt [Li(bpzcp)(THF)][23,24b] with NH_4Cl/H_2O in diethyl ether[21,22] cleanly afforded the two previously described scorpionate/cyclopentadiene regioisomers[25a] (bpzcpH) 1-[2,2-bis(3,5-dimethylpyrazol-1-yl)-1,1-diphenylethyl]-1,3-cyclopentadiene (**a**) and 2-[2,2-bis(3,5-dimethylpyrazol-1-yl)-1,1-diphenylethyl]-1,3-cyclopentadiene (**b**) in very good yields (Scheme 1b). Additionally, derivative **3** could be only prepared by reacting bpzcpH with the bisalkyl $Mg(^nBu)_2$ (Scheme 1c).

Alternatively, subsequent reaction of the bpzcpH ligand with ZnR_2 (1 equiv vs Zn) at low temperature (−70 °C) in toluene cleanly afforded the corresponding zinc complexes [Zn(R){κ^2-$\eta^1(\pi)$-bpzcp}] (R = Me **7**, Et **8**, ^{t}Bu **9**, CH_2SiMe_3**10**) in very good yields (>75%) as brown microcrystalline powders (Scheme 2a). Furthermore, inspired by Carmona's work,[27a] we successfully proved that the use of alkyl magnesium complexes **1**, **2**, **4**, and **5** enabled excellent cyclopentadienyl and alkyl transfers to the zinc metal center and allowed the formation of derivatives **7**−**10** in good isolated yields (Scheme 2b). Compounds **1**−**10** are extremely air- and moisture-sensitive, are highly soluble in tetrahydrofuran (THF), toluene, and diethyl ether, but sparingly soluble in *n*-hexane − apart from derivatives with R = ^{n}Bu, ^{t}Bu, and CH_2SiMe_3. All compounds decompose in dichloromethane. Qualitative

(25) (a) Otero, A.; Fernández-Baeza, J.; Antiñolo, A.; Lara-Sánchez, A.; Martínez-Caballero, E.; Tejeda, J.; Sánchez-Barba, L. F.; Alonso-Moreno, C.; López-Solera, I. *Organometallics* **2008**, *27*, 976–983. (b) Otero, A.; Fernández-Baeza, J.; Lara-Sánchez, A.; Antiñolo, A.; Tejeda, J.; Martínez-Caballero, E.; Márquez-Segovia, I.; López-Solera, I.; Sánchez-Barba, L. F.; Alonso Moreno, C. *Inorg. Chem.* **2008**, *47*, 4996–5005.

(26) (a) Kunz, K.; Bolte, M.; Lerner, H.-W.; Wagner, M. *Organometallics* **2009**, *28*, 3079–3087. (b) Kunz, K.; Vitze, H.; Bolte, M.; Lerner, H. W.; Wagner, M. *Organometallics* **2007**, *26*, 4663–4672. (c) Lopes, I.; Lin, G. Y.; Domingos, A.; McDonald, R.; Marques, N.; Takats, J. *J. Am. Chem. Soc.* **1999**, *121*, 8110–8111.

(27) (a) Fernández, R.; Grirrane, A.; Resa, I.; Rodríguez, A.; Carmona, E.; Álvarez, E.; Gutierrez-Puebla, E.; Monge, A.; López del Amo, J. M.; Limbach, H.-H.; Lledós, A.; Masera, F.; del Río, D. *Chem.—Eur. J.* **2009**, *15*, 924–935. (b) Walker, D. A.; Woodmann, T. J.; Schormann, M.; Hughes, D. L.; Bochmann, M. *Organometallics* **2003**, *22*, 797–803.

(28) (a) Hanusa, T. P. *Organometallics* **2002**, *21*, 2559–2571. (b) Jutzi, P.; Burford, N. *Chem. Rev.* **1999**, *99*, 969–990. (c) El-Kaderi, H. M.; Xia, A.; Heeg, M. J.; Winter, C. H. *Organometallics* **2004**, *23*, 3488–3495. (d) Xia, A.; Knox, J. E.; Heeg, M. J.; Schlegel, H. B.; Winter, C. H. *Organometallics* **2003**, *22*, 4060.

Scheme 2. Synthesis of Scorpionate/Cyclopentadienyl Zinc Alkyls [Zn(R){κ^2-η^1(π)-bpzcp}] (**7**−**10**)

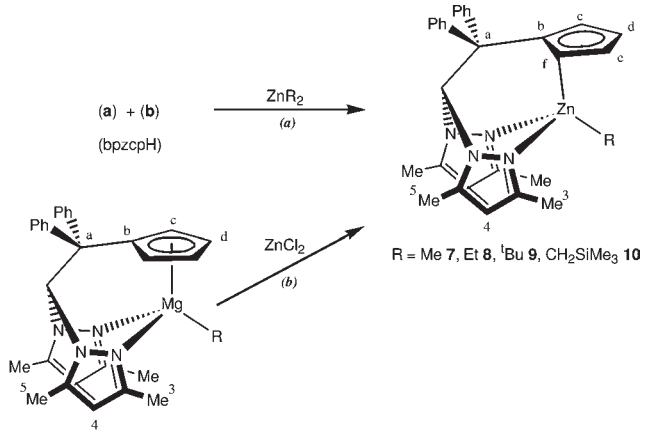

tests on complexes **1**−**6** showed the absence of halide through the formation of a [MgCl(κ^2-η^5-bpzcp)] derivative.

The ^{1}H and ^{13}C-{^{1}H} NMR spectra of **1**−**10** in benzene-d_6 at room temperature display a singlet for the H^4, Me^3, and Me^5 pyrazole protons, indicating that both pyrazoles are equivalent, along with two multiplets for the cyclopentadienyl protons (H^c and H^d) and one resonance for the alkyl ligands. The pattern corresponding to the cyclopentadienyl fragment remains unchanged down to −80 °C, and this clearly suggests that a very fast haptotropic exchange[27b] takes place in solution for the alkyl zinc derivatives (**7**−**10**), even at the lowest temperature investigated, since it is well established that these systems present a η^1(π)-C_5H_4-coordination mode to the zinc metal center in the solid state. This situation has been observed previously by Carmona et al. in beryllocenes and zincocenes with substituted and unsubstituted cyclopentadienyl rings.[27a] Such systems are well-known to exhibit dynamic behavior both in solution[29] and in the solid state.[30] All of these data indicate that "*in solution*" in the zinc complexes the metal atom adopts a tetrahedral disposition, as a result of this haptotropic exchange,[27b] a symmetry plane exists and contains the metal center, the bridging carbon of the pyrazole rings, and the C^a and C^b atoms from the cyclopentadienyl fragment (Schemes 1 and 2). The phase-sensitive ^{1}H NOESY-1D spectra were also obtained to confirm the assignments of the signals for H^c and H^d from the cyclopentadienyl group and Me^3 and Me^5 from the pyrazole rings.

Complexes **4**, **5**, **7**, and **10** × **0.5C$_7$H$_8$** were characterized by single-crystal X-ray diffraction. Selected bond lengths and angles are collected in Tables 1 and 2. Crystallographic details are reported in Table 5, and the molecular structures are illustrated in Figures 1−4, respectively. All complexes present a monomeric structure in the solid state, and the metal centers exhibit a distorted tetrahedral geometry, in which the pyrazolic nitrogens N(1) and N(3) occupy two positions and the alkyl group and the cyclopentadienyl fragment the other two positions.

The molecular structures of **4** and **5** are presented in Figures 1 and 2, respectively, and show a distortion of the tetrahedral geometry of the metal center because of the scorpionate ligand, which acts in a κ^2-NN-η^5-C_5H_4 coordination mode with the Mg(1) atom 0.883(2) Å and

Table 1. Selected Interatomic Distances (Å) and Angles (deg) for **4** and **5**

	4	**5**
Bond Distances (Å)		
Mg(1)−N(1)	2.208(4)	2.20(1)
Mg(1)−N(3)	2.223(4)	2.22(1)
Mg(1)−C(13)	2.179(4)	2.15(1)
Mg(1)−C(21)	2.442(4)	2.44(1)
Mg(1)−C(22)	2.507(4)	2.48(1)
Mg(1)−C(23)	2.543(4)	2.54(1)
Mg(1)−C(24)	2.489(4)	2.53(1)
Mg(1)−C(25)	2.423(4)	2.46(1)
C(1)−C(2)	1.587(6)	1.61(1)
C(1)−C(21)	1.536(5)	1.54(1)
C(21)−C(22)	1.404(6)	1.44(2)
C(21)−C(25)	1.421(5)	1.42(1)
C(22)−C(23)	1.396(5)	1.40(1)
C(23)−C(24)	1.406(6)	1.40(1)
C(24)−C(25)	1.408(6)	1.36(1)
Bond Angles (deg)		
N(1)−Mg(1)−N(3)	83.6(1)	82.6(4)
N(1)−Mg(1)−C(13)	113.5(1)	110.5(4)
N(3)−Mg(1)−C(13)	115.5(2)	107.2(4)
Cent(1)−Mg(1)−N(1)	106.4	105.5
Cent(1)−Mg(1)−N(3)	102.9	106.0
Cent(1)−Mg(1)−C(13)	126.4	133.3
C(2)−C(1)−C(21)	111.5(3)	115.3(8)

Table 2. Selected Interatomic Distances (Å) and Angles (deg) for **7** and **10**

	7	**10**
Bond Distances [Å]		
Zn(1)−N(1)	2.099(7)	2.104(6)
Zn(1)−N(3)	2.094(6)	2.171(6)
Zn(1)−C(14)	2.137(8)	2.166(7)
Zn(1)−C(13)	2.74(1)	2.787(2)
Zn(1)−C(15)	2.81(1)	2.659(1)
Zn(1)−C(16)	3.51(1)	3.015(1)
Zn(1)−C(17)	3.48(1)	3.414(2)
Zn(1)−C(30)	1.966(8)	1.985(7)
C(11)−C(12)	1.60(1)	1.61(1)
C(13)−C(14)	1.47(1)	1.43(1)
C(13)−C(17)	1.36(1)	1.38(1)
C(14)−C(15)	1.44(1)	1.42(1)
C(15)−C(16)	1.36(1)	1.38(1)
C(16)−C(17)	1.42(1)	1.41(1)
Bond Angles (deg)		
N(1)−Zn(1)−N(3)	83.9(2)	88.6(2)
N(1)−Zn(1)−C(30)	118.6(3)	114.6(3)
N(3)−Zn(1)−C(30)	118.7(3)	112.7(3)
N(1)−Zn(1)−C(14)	88.4(3)	100.1(2)
N(3)−Zn(1)−C(14)	108.4(3)	87.7(3)
C(14)−Zn(1)−C(30)	126.8(4)	139.3(3)
C(11)−C(12)−C(13)	115.4(6)	113.4(5)
Zn(1)−C(14)−C(13)	97.3(5)	99.6(4)
Zn(1)−C(14)−C(15)	101.8(6)	93.5(5)
Zn(1)−C(14)−plane of ring	105.2	96.46
Zn(1)−C(30)−Si(1)		118.2(4)

(29) (a) Wang, H.; Kehr, G.; Fröhlich, R.; Erker, G. *Angew. Chem.* **2007**, *119*, 4992–4995. *Angew. Chem., Int. Ed.* **2007**, *46*, 4905−4908.(b) Carmona, E.; Fernández, R. *Eur. J. Inorg. Chem.* **2005**, 3197–3206. (c) Conejo, M. M.; Fernández, R.; del Río, D.; Carmona, E.; Monge, A.; Ruiz, C.; Márquez, A. M.; Sanz, J. F. *Chem.—Eur. J.* **2003**, *9*, 4452–4461. (d) Fischer, B.; Wijkens, P.; Boersma, J.; van Koten, G.; Smeets, W. J. J.; Spek, A. L.; Budzelaar, P. H. M. *J. Organomet. Chem.* **1989**, *376*, 223–233.

(30) (a) Lopez del Amo, J. M.; Buntkowsky, G.; Limbach, H. H.; Resa, I.; Fernandez, R.; Carmona, E. *J. Phys. Chem. A* **2008**, *112*, 3557–3565. (b) Hung, I.; Macdonald, C. L. B.; Schurko, R. W. *Chem.—Eur. J.* **2004**, *10*, 5923–5935.

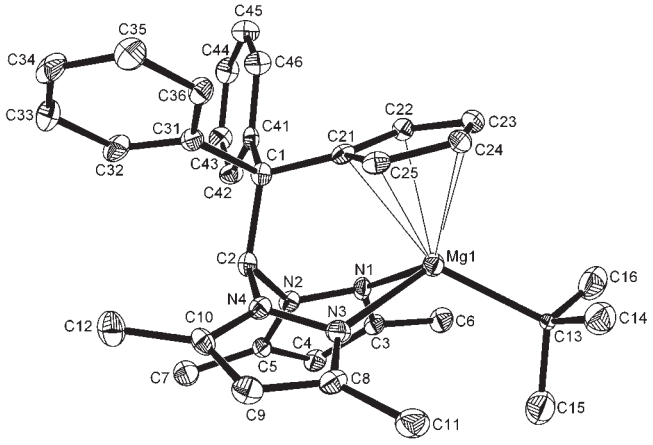

Figure 1. ORTEP view of [Mg(ᵗBu)(κ^2-η^5-bpzcp)] (**4**). Hydrogen atoms have been omitted for clarity. Thermal ellipsoids are drawn at the 30% probability level.

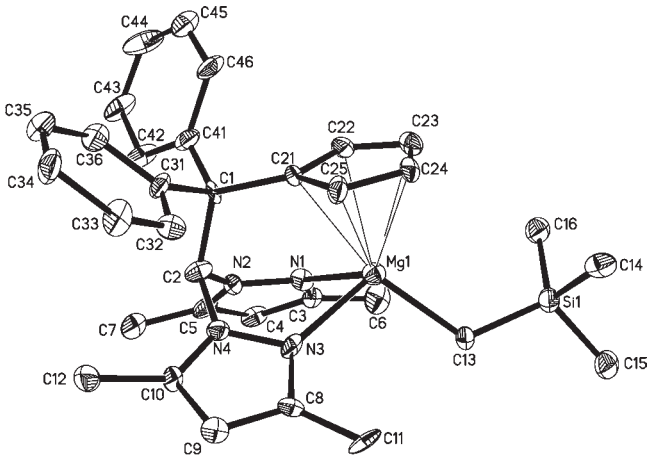

Figure 2. ORTEP view of [Mg(CH_2SiMe_3)(κ^2-η^5-bpzcp)] (**5**). Hydrogen atoms have been omitted for clarity. Thermal ellipsoids are drawn at the 30% probability level.

−0.996(6) Å out of the plane defined by N(1)−N(3)−C(13) for **4** and **5**, respectively. The N(1)−Mg and N(3)−Mg bond lengths are well-balanced at 2.208(4) Å and 2.223(4) Å for complex **4**, and 2.20(1) Å and 2.22(1) Å for complex **5** (Table 1). The four-membered Mg−C(1)−C(2)−C(21) fragment and the alkyl group lie around a pseudo-mirror plane that shows the symmetry in the molecule.

The solid-state structures also reveal that the C_5H_4 fragment is coordinated in a pentahapto fashion to the magnesium atom, a situation that has been previously observed in several complexes[23−25] synthesized in our group and supported with this hybrid ligand. Delocalization is also evidenced in the C_5H_4 ring, with the C−C bond lengths ranging on average from 1.396(5) Å to 1.421(5) Å for derivative **4**, and from 1.36(1) Å to 1.44(2) Å for derivative **5** (Table 1). The C_5H_4 ring is unsymmetrically bonded to the Mg atom, with Mg−C bond lengths ranging from 2.423(4) to 2.543(4) Å for **4**, and from 2.44(1) to 2.54(1) Å for **5** (Table 1). Finally, the alkyl moiety is directly bonded to the Mg center with a Mg−C(13) bond length of 2.179(4) Å for **4** and 2.15(1) Å for **5** (Table 1); the bond in **5** is shorter than that in **4** as a result of steric hindrance because of the *tert*-butyl group.

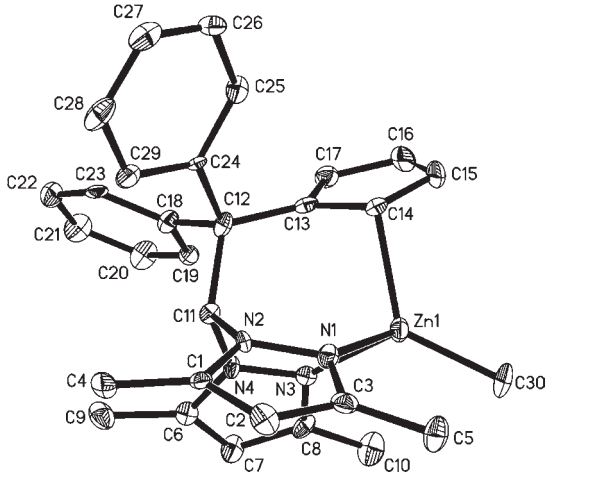

Figure 3. ORTEP view of [Zn(CH_3){κ^2-η^1(π)-bpzcp}] (**7**). Hydrogen atoms have been omitted for clarity. Thermal ellipsoids are drawn at the 30% probability level.

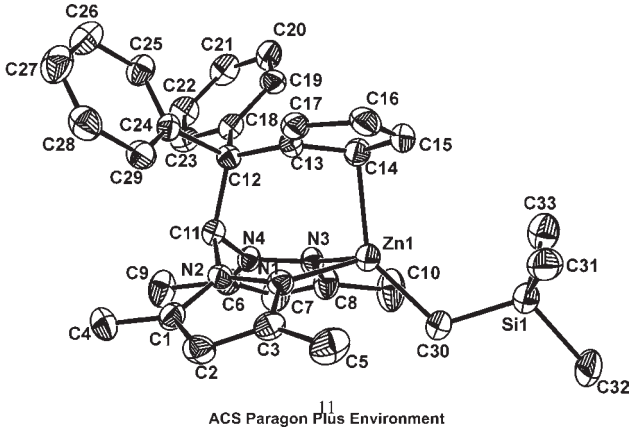

Figure 4. ORTEP view of [Zn(CH_2SiMe_3){κ^2-η^1(π)-bpzcp}] (**10** × **0.5C_7H_8**). Hydrogen atoms have been omitted for clarity. Thermal ellipsoids are drawn at the 30% probability level.

The most notable feature in the X-ray molecular structures of complexes **7** and **10** (Figures 3 and 4, respectively) is undoubtedly the peripheral $\eta^1(\pi)$ coordination mode of the cyclopentadienyl ring. In this situation, the cyclopentadienyl fragment maintains partial aromatic character, with C−C bond lengths ranging from 1.36(1) Å to 1.47(1) Å for complex **7**, and from 1.38(1) Å to 1.43(1) Å for complex **10**, clearly in the range between simple and double bonds. For instance, the difference between the $C_\beta C_\beta$ and $C_\alpha C_\beta$ bonds [α and β refer to the positions with respect to C(14), that is, the four coordinated carbon of the $\eta^1(\pi)$ ring] is 0.06 Å in **7** and 0.03 Å in **10**. The calculated difference in similar zincocenes with one of the two $C_5Me_4(SiMe_3)$ moieties in a $\eta^1(\pi)$-coordination mode is also 0.07 Å,[31a] while in $[B(C_5Me_5)_2]^+$ it has double that value, that is, 0.14 Å, in agreement with a localized structure.[31b]

(31) (a) Fernández, R.; Resa, I.; del Río, D.; Carmona, E. *Organometallics* **2003**, *22*, 381–383. (b) Voigt, A.; Filipponi, S.; Macdonald, C. L. B.; Gorden, J. D.; Cowley, A. H. *Chem. Commun.* **2000**, 911–912. (c) Burkey, D. J.; Hanusa, T. P. *J. Organomet. Chem.* **1996**, *512*, 165–173. (d) Data taken from a computer search at the CCDC.(e) Cordero, B.; Gómez, V.; Platero-Prats, A. E.; Revés, M.; Echeverría, J.; Cremades, E.; Barragán, F.; Álvarez, S. *Dalton Trans.* **2008**, 2832–2838.

Additionally, the Zn(1)−C(14) bond length of 2.137(8) Å for **7** and 2.166(7) Å for **10**, as well as the angle of about 105.2° for **7** and 96.46° for **10** formed by the Zn(1)−C(14) bond with the plane of this ring, are typical for this type of $\eta^1(\pi)$-coordination mode.[27,31c,32] As a comparison, the C(14)−Zn distance of 2.166(7) Å in **10**, although shorter than the corresponding average distance in C(21−25)−Mg [2.490(3) Å] in **5**, evidence the higher C−M bond strength in the former and is well above the average for Zn−C covalent bonds[31d] [ca. 2.005(3) Å] and 0.23 Å longer than the 1.930(2) Å distance found for the Zn−C σ-bond in dimethylzinc.[33]

In a similar way to the magnesium crystal structures, the alkyl moiety is directly bonded to the Zn center with a Zn−C(30) bond length of 1.966(8) Å in complex **7** and 1.985(7) Å in complex **10** (Table 2).

Finally, comparison between the trimethylsilylmethyl magnesium and zinc derivatives **5** and **10** reveals that the M−C alkyl bond length in complex **10** [1.985(7) Å] is shorter than that in complex **5** [2.15(1) Å]. This situation is probably the result of the higher magnesium covalent radius (1.41 Å) in comparison with the zinc one (1.22 Å);[31e] however, electronic effects derived from the $\eta^1(\pi)$-coordination mode of the C_5H_4 ring in the zinc compound **10** can neither be discarded.

Synthesis and Characterization of Scorpionate/Cyclopentadienyl Zinc and Magnesium Chloride, Amide, and Alkoxide Complexes. Given the interest in amide[34] and alkoxide[34b,35] complexes for the ROP of cyclic esters, and considering our previous experience in the preparation of analogous heteroscorpionate zinc chloride[22] derivatives as convenient starting materials for the preparation of alkoxide and amide complexes, we decided to react the scorpionate/cyclopentadienyl hybrid ligand in the form of the lithium salt[23,24b] with $ZnCl_2$ (1 equiv vs Zn) at low temperature to afford cleanly the corresponding chloride complex [ZnCl{κ^2-$\eta^1(\pi)$-bpzcp}] (**11**) in very good yield (> 75%) as a white microcrystalline powder (Scheme 3a). The heteroscorpinate chloride **11** is extremely air- and moisture-sensitive, is soluble in THF but sparingly soluble in toluene and diethyl ether, and insoluble in *n*-hexane.

Subsequent reaction of the monochloride zinc species **11** with an aromatic (primary)amide lithium salt in toluene at room temperature afforded the corresponding scorpionate/cyclopentadienyl amide complex of the type [Zn(NH-4-MeC_6H_4){κ^2-$\eta^1(\pi)$-bpzcp}] (**12**) (NH-4-MeC_6H_4 = 4-methylphenylamide) (Scheme 3b). Attempts to synthesize aliphatic amide derivatives employing the zinc chloride precursor **11** failed and produced intractable mixtures, as previously observed for the preparation of amidinate-heteroscorpionate amide zinc complexes.[22]

Scheme 3. Synthesis of the Scorpionate/Cyclopentadienyl Zinc Chloride [ZnCl{κ^2-$\eta^1(\pi)$-bpzcp}] (**11**) and Amide Complex [Zn(NH-4-MeC_6H_4){κ^2-$\eta^1(\pi)$-bpzcp}] (**12**)

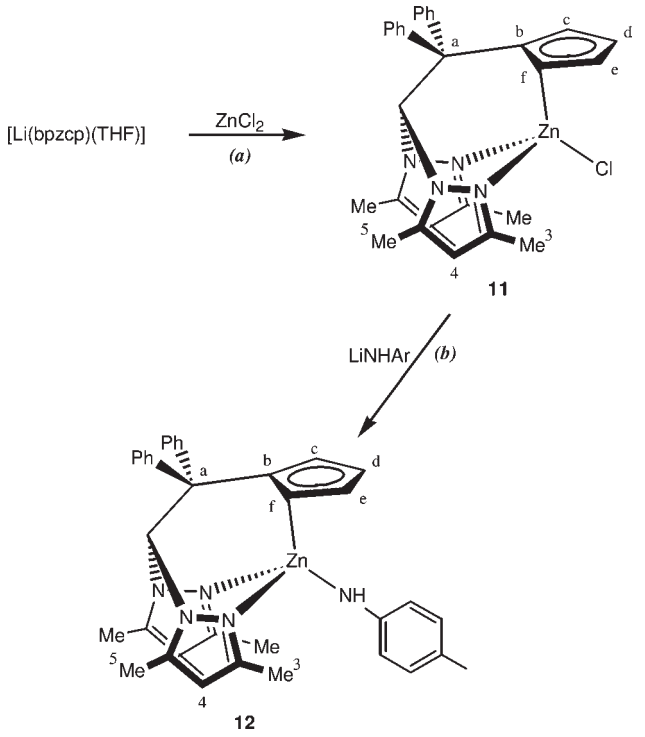

Scheme 4. Synthesis of the Scorpionate/Cyclopentadienyl Zinc Amide and Alkoxide Complexes [Zn(R){κ^2-$\eta^1(\pi)$-bpzcp}] (**13**−**14**) and the Magnesium Amide [Mg{$N(SiMe_3)_2$}{κ^2-η^5-bpzcp)] (**15**)

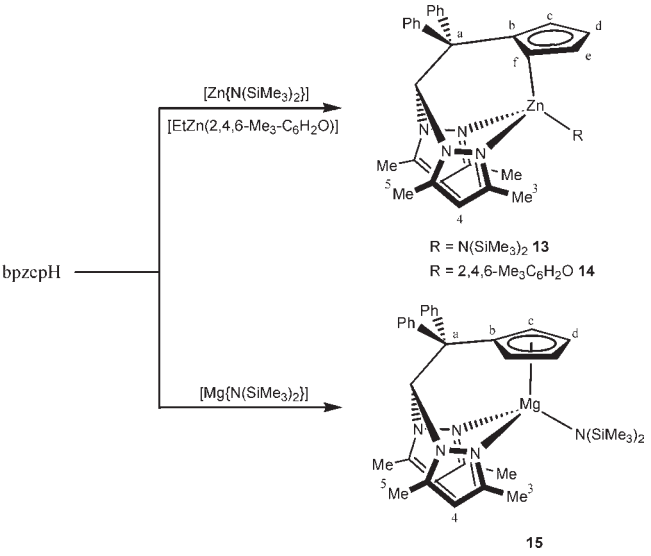

In an effort to prepare aliphatic amide and alkoxide species analogous to **12**, we employed an alternative route that involved a protonolysis reaction of the corresponding bis-amides [M{$N(SiMe_3)_2$}$_2$] (M = Mg, Zn) and the alkoxo-ethyl zinc mixed-ligand complex [EtZn(2,4,6-$Me_3C_6H_2O$)] (2,4,6-$Me_3C_6H_2O$ = mesityloxy) with the hybrid ligand bpzcpH (Scheme 4). Thus, the reaction of bpzcpH with the amide and alkoxide starting materials

(32) (a) Darensbourg, D. J.; Wildeson, J. R.; Yarbrough, J. C. *Organometallics* **2001**, *20*, 4413–4417. (b) Blom, R.; Boersma, J.; Budzelaar, P. H. M.; Fischer, B.; Haalan, A.; Volden, H. V.; Weidlein, J. *Acta Chem. Scand. Ser. A* **1986**, *40*, 113–120. (c) Fischer, B.; Wijkens, P.; Boersma, J.; van Koten, G.; Smeets, W. J. J.; Spek, A. L.; Budzelaar, P. H. M. *J. Organomet. Chem.* **1989**, *376*, 223–233.

(33) Almenningen, A.; Helgaker, T. U.; Haaland, A.; Samdal, S. *Acta Chem. Scand.* **1982**, *A36*, 159.

(34) (a) Chisholm, M. H.; Gallucci, J. C.; Phomphrai, K. *Inorg. Chem.* **2005**, *44*, 8004–8010. (b) Chisholm, M. H.; Gallucci, J.; Phomphrai, K. *Inorg. Chem.* **2002**, *41*, 2785–2794. (c) Cheng, M.; Moore, D. R.; Reczek, J. J.; Chamberlain, B.; Lobkovsky, E. B.; Coates, G. W. *J. Am. Chem. Soc.* **2001**, *123*, 8738–8749.

(35) (a) Chisholm, M. H.; Gallucci, J. C.; Phomphrai, K. *Inorg. Chem.* **2004**, *43*, 6717–6725. (b) Rieth, L. R.; Moore, D. R.; Lobkovsky, E. B.; Coates, G. W. *J. Am. Chem. Soc.* **2002**, *124*, 15239–15248. (c) Chisholm, M. H.; Gallucci, J. C.; Zhen, H.; Huffman, J. C. *Inorg. Chem.* **2001**, *40*, 5051–5054.

Table 3. Polymerization of ε-Caprolactone Catalyzed by Complexes **1**, **4**, **5**, **7**, **9**, and **10**[a]

entry	initiator	temp (°C)	time (h)	yield (g)	conv (%)[b]	prod[c]	M_n (Da)[d]	M_w/M_n[d]
1	**1**	20	18	2.90	56	2	30 200	1.38
2	**4**	20	18	3.70	72	2	39 500	1.39
3	**4**	70	2	4.90	95	27	53 200	1.49
4	**5**	20	1 (min)	4.71	92	3 139	51 800	1.19
5	**5**	0	2	1.24	24	7	12 800	1.08
6	**5**[e]	20	10 (min)	7.41	65	2 223	151 000	1.45
7	**[Mg(CH$_2$SiMe$_3$)(tbpamd)]**[f]	20	1 (min)	4.98	97	3 320	36 900	1.41
8	**7**	80	48	2.60	51	0.6	27 200	1.53
9	**9**	80	48	3.20	62	0.7	33 700	1.49
10	**10**	80	18	3.30	64	2	34 600	1.33
11	**10**	20	48	traces				
12	**[Zn(CH$_2$SiMe$_3$)(tbpamd)]**[f]	20	15	1.19	24	1	18 600	1.09

[a] Polymerization conditions: 90 μmol of initiator, 20 mL of toluene as solvent, $[\varepsilon\text{-CL}]_0/[\text{initiator}]_0 = 500$. [b] Percentage conversion of the monomer [(weight of polymer recovered/weight of monomer) × 100]. [c] kg polymer × [mol of metal (Mg/Zn)]$^{-1}\cdot$h^{-1}. [d] Determined by GPC relative to polystyrene standards in THF. Experimental M_n was calculated considering Mark−Houwink's corrections[48] for M_n [M_n(obsd) = 0.56· × M_n(GPC)]. [e] 20 μmol of initiator, 30 mL of toluene as solvent, $[\varepsilon\text{-CL}]_0/[\text{initiator}]_0 = 5000$. [f] These data have been included for comparison in ROP with the alkyl magnesium[20] and zinc[21] analogues.

(1 equiv vs M) at low temperature (−70 °C) in toluene cleanly afforded the corresponding monoamide/alkoxide scorpionate/cyclopentadienyl complexes [Zn(R){κ^2-η^1(π)-bpzcp}] (R = N(SiMe$_3$)$_2$ **13**, R = 2,4,6-Me$_3$C$_6$H$_2$O **14**) and [Mg{N(SiMe$_3$)$_2$}(κ^2-η^5-bpzcp)] (**15**) in very good yields (>80%) as brown and white microcrystalline powders, respectively.

The ^{1}H and ^{13}C-{^{1}H} NMR spectra of **11**−**15** in benzene-d_6 at room temperature display a single set of resonances for the Me^5 and Me^3 groups from both pyrazole rings, indicating their equivalence, and for the bridging CH, along with two multiplets for the cyclopentadienyl protons (H^c and H^d). Additionally, ^{1}H NOESY-1D experiments were also performed to confirm the assignment of the signals for the Me$^{3\text{ or }5}$ groups of the pyrazole rings as well as for H^c and H^d in the cyclopentadienyl fragment. These data suggest a tetrahedral disposition *in solution* for the metal center. In this arrangement a plane of symmetry exists for both the pyrazole rings and the C_5H_4 fragment, and this contains both the metal center and the chloride, amide, or alkoxide ligand (Schemes 3 and 4). As discussed above, zinc complexes **11**−**14** show an unchanged pattern corresponding to the cyclopentadienyl fragment down to −80 °C. This finding is due to the fast haptotropic exchange[27b] in solution. In a similar way to the zinc alkyls **7**−**10**, in the solid state a η^1(π)-C_5H_4 arrangement is assumed for complexes **11**−**14**, although unfortunately evidence for this proposal could not be obtained by X-ray analysis.

Polymerization Studies on Scorpionate/Cyclopentadienyl Magnesium and Zinc Alkyl, Amide, and Alkoxide Complexes with ε-Caprolactone and Lactides. Complexes **1**, **4**, **5**, **7**, **9**, **10**, **13** and **14** were assessed in the ROP of the polar monomers ε-caprolactone (CL) and L-/*rac*-lactide (L-LA, *rac*-LA) to probe their potential as initiators for cyclic esters. These reactivity studies also allowed a comparison of the Mg-alkyl relative to Zn-alkyl moieties as initiating groups in these hybrid scorpionate/cyclopentadienyl alkyl systems.

***ε*-Caprolactone Polymerization Promoted by Scorpionate/Cyclopentadienyl Alkyl Magnesium and Zinc Complexes.** Initiators **1**, **4**, **5**, **7**, **9**, and **10** act as efficient single-component catalysts for the polymerization of ε-caprolactone (CL) to give high molecular weight polymers; the results of these experiments are collected in Table 3. A variety of polymerization conditions were explored. The magnesium alkyl derivatives **1** and **4** effectively polymerize CL at room temperature (entries 1 and 2) and **4** gives rise to 72% of conversion of 500 equiv of CL after 18 h. The polymerization is well controlled and gives a high molecular weight polymer with a medium broad polydispersity (M_n = 39 500, M_w/M_n = 1.39). Not unexpectedly, an increase in the temperature up to 70 °C led to complete conversion of the monomer in 2 h without a notable increase in the polydispersity index (M_w/M_n = 1.49, entry 3), showing a higher productivity [27 × 10^3 g PCL (mol Mg)$^{-1}\cdot$h^{-1}]. Surprisingly, magnesium alkyl **5** initiates very rapid polymerization at room temperature, accompanied by a marked increase in the viscosity of the solution, and gives almost complete conversion in 1 min with a productivity of more than 3 139 × 10^3 g PCL (mol Mg)$^{-1}\cdot$h^{-1} (entry 4). This activity is retained at 0 °C (entry 5) and after 2 h 24% of the monomer was converted with a narrow molecular weight distribution, which suggests living behavior (M_w/M_n = 1.08, entry 5). Alkyl magnesium **5** shows an extraordinarily high activity, which is comparable to the previously described amidinate-based alkyl magnesium initiator [Mg(CH$_2$SiMe$_3$)-(tbpamd)][20] (entry 7).

As a comparison, alkyl zinc initiators **7**, **9**, and **10** showed significantly lower activity than the analogous heteroscorpionate amidinate-based alkyl zinc derivatives recently reported by our group[21] (Table 3, entry 12). For instance, **9** and **10** polymerize CL effectively at 80 °C (entries 9 and 10) and in the case of **10** 64% of the monomer was transformed after 18 h to produce medium-high molecular weight materials with a medium-broad polydispersity index (entry 10, M_n = 34 600, M_w/M_n = 1.33). The productivity decreases markedly on cooling, and in the reaction at 20 °C, the catalytic activity of **10** is drastically reduced and only traces of product are formed (entry 11).

In these tests the polymer molecular weights were limited by the monomer/initiator ratio of 500:1. An increase in this ratio by a factor of 10 gave polymers with significantly higher molecular weight ($M_n > 10^5$) and broader molecular weight distribution (entry 6, M_w/M_n = 1.45), possibly because of the occurrence of backbiting as well as transesterification as side reactions, resulting in the formation of

Table 4. Polymerization of L-Lactide and *rac*-Lactide Catalyzed by Complexes **5**, **10**, **13**, and **14**[a]

entry	initiator	monomer	temp (°C)	time (h)	yield (g)	conv (%)[b]	$M_{n(theor.)}$ (Da)[c]	M_n(Da)[d]	M_w/M_n[d]	T_m(°C)[e]	$[\alpha]_D^{22}$ (deg)[f]
1	**5**	L-LA	90	0.5	0.59	23	6 600	5 800	1.03	161	−146
2	**5**	L-LA	90	1	1.06	41	11 800	11 400	1.02	160	−147
3	**5**	L-LA	90	1.5	1.50	58	16 700	16 500	1.02	165	−148
4	**5**	L-LA	90	2	2.05	79	22 700	22 500	1.03	165	−145
5	**5**	L-LA	90	2.5	2.51	97	27 900	27 600	1.05	164	−146
6	**5**	L-LA	65(THF)	5	1.81	70	20 100	21 100	1.15	165	−149
7	**5**	L-LA	bulk	0.5	2.09	81	23 300	22 200	1.38	155	−155
8	[**Mg(CH$_2$SiMe$_3$)-(pbpamd)**][g]	L-LA	70	96	1.20	93	13 400	12 600	1.19	160	−146
9	**10**	L-LA	90	30	2.09	81	23 300	21 000	1.18	160	−153
10	**13**	L-LA	90	72							
11	**14**	L-LA	90	18	2.40	92	26 500	21 500	1.19	165	−146
12	**5**	*rac*-LA	90	4	0.82	32	9 200	8 800	1.07	126	
13	**5**	*rac*-LA	90	8	1.52	59	17 000	15 500	1.12	127	
14	**5**	*rac*-LA	bulk	2	1.06	41	11 800	10 900	1.41	135	

[a] Polymerization conditions: 90 μmol of initiator; 70 mL of toluene as solvent, $[\text{L-lactide}]_0/[\text{initiator}]_0 = 200$ and $[\textit{rac}\text{-LA}]_0/[\text{initiator}]_0 = 200$. [b] Percentage conversion of the monomer [(weight of polymer recovered/weight of monomer) × 100]. [c] Theoretical M_n = (monomer/initiator) × (% conversion) × (M_w of lactide). [d] Determined by GPC relative to polystyrene standards in THF. Experimental M_n was calculated considering Mark−Houwink's corrections[48] for M_n [M_n(obsd) = 0.56 × M_n(GPC)]. [e] PLA melting temperature. [f] Optical rotation data of poly(L-lactide) obtained. $[\alpha]_D^{22}$ of L-lactide and poly(L-lactide) are −285° and −144°, respectively.[17d] [g] These data have been included for comparison in ROP with the alkyl magnesium analogues,[20] 90 μmol of initiator; $[\text{L-lactide}]_0/[\text{initiator}]_0 = 100$.

macrocycles with a wide range of molecular weight distributions. The lower M_n values (as compared to those expected for a well-controlled polymerization) observed in all cases (entries 1−6) are also indicative of transfer reactions. In accordance with the aforementioned data, it is worth noting that the polymerization processes initiated by alkyl zinc initiators **7**, **9**, and **10** are significantly slower than those initiated by their alkyl magnesium counterparts **1**, **4**, and **5**. This marked difference between the two types of derivatives, which under the present polymerization conditions decreases in the order [**Mg(R)**(κ^2-η^5-**bpzcp**)] ≫ [**Zn(R)**{κ^2-η^1(π)-**bpzcp**}], is presumably a consequence of the M−C bond strength; this trend is consistent with the decrease in the lability of the M−C bond[36]and may rationalize the delay in the initiation step observed on employing these zinc initiators. Additionally, the nature of the alkyl group in both families of initiators affects the catalytic activity, which decreases in the order **CH$_2$SiMe$_3$** ≫ **^{t}Bu** > **Me**, and is also in agreement with the decrease in the lability of the M−C bond.[36] This behavior has also been observed in analogous amidinate-based magnesium[20] and zinc alkyl[21]/amide[22] derivatives.

The ^{1}H NMR spectrum of poly(ε-caprolactone) oligomer, derived from the reaction of **5** with 25 equiv of ε-CL exhibits characteristic resonances that are consistent with the presence of one −CH$_2$SiMe$_3$ end group per CH$_2$OH hydroxyl chain end. This provides evidence confirming that the polymerization follows a nucleophilic route and is initiated by the transfer of an alkyl ligand to the monomer, with cleavage of the acyl-oxygen bond and formation of a metal alkoxide-propagating species.[37] Very few alkyl magnesium and zinc initiators[38] have been shown to polymerize ε-caprolactone to medium molecular weight polymers. By contrast, catalysts **5** and **10**, as well as analogous alkyl magnesium[20] and alkyl[21]/amide[22] zinc initiators described by our group, have proved to be efficient initiators for the production of medium-high molecular weight polymers with medium-broad molecular weight distributions, even at a catalyst loading of 0.08%, which yielded M_n values as high as 151 kg·mol^{-1} (entry 6).

L- and *rac*-Lactide Polymerization Initiated by Scorpionate/Cyclopentadienyl Alkyl Complexes. Derivatives **5**, **10**, **13**, and **14** were also examined for the production of PLAs (Table 4). Complex **5** proved to be an active catalyst for the polymerization of L-lactide at 90 °C in toluene without co-catalyst or activator (Table 4, entries 1−5). In all cases, the PLAs produced have molecular weights in close agreement with calculated values for one polymer chain per metal center [M_n(calcd)PLA$_{200}$ = 28 800] (Table 4). The gel permeation chromatography (GPC) data for the resulting polyesters show a monomodal weight distribution, with polydispersities ranging from 1.02 to 1.05. At this point, it is worth mentioning that polymerization of the optically active (*S*,*S*)-lactide (L-lactide) afforded 58% conversion of 200 equiv in 1.5 h, with a very narrow molecular weight distribution (M_w/M_n = 1.02, entry 3). On extending the reaction time up to 2.5 h, 97% of the monomer was transformed without an appreciable increase in the molecular weight distribution (M_w/M_n = 1.05, entry 5). The polymerization occurs without observable epimerization reactions at the chiral centers, as evidenced by the homonuclear decoupled ^{1}H NMR spectrum, which has only a single resonance at δ 5.16 ppm in the methine region, affording highly crystalline, isotactic polymers with a T_m in the range of 160−165 °C.[39] The low level of stereochemical imperfections is also revealed in the poly(L-lactide) with M_n > 25 000, for which the

(36) Martinho, J. A.; Beauchamp, J. L. *Chem. Rev.* **1990**, *90*, 629–688.
(37) (a) Sánchez-Barba, L. F.; Hughes, D. L.; Humphrey, S. M.; Bochmann, M. *Organometallics* **2006**, *25*, 1012–1020. (b) Sánchez-Barba, L. F.; Hughes, D. L.; Humphrey, S. M.; Bochmann, M. *Organometallics* **2005**, *24*, 5329–5334. (c) Sánchez-Barba, L. F.; Hughes, D. L.; Humphrey, S. M.; Bochmann, M. *Organometallics* **2005**, *24*, 3792–3799.
(38) (a) Sarazin, Y.; Howard, R. H.; Hughes, D. L.; Humphrey, S. M.; Bochmann, M. *Dalton Trans.* **2006**, 340–350. (b) Sarazin, Y.; Schormann, M.; Bochmann, M. *Organometallics* **2004**, *23*, 3296–3302. (c) Walker, D. A.; Woodman, T. J.; Schormann, M.; Hughes, D. L.; Bochmann, M. *Organometallics* **2003**, *22*, 797–803.
(39) (a) Radano, C. P.; Baker, G. L.; Smith, M. R. *J. Am. Chem. Soc.* **2000**, *122*, 1552–1553. (b) Zhong, Z.; Dijkstra, J. P.; Feijen, J. *J. Am. Chem. Soc.* **2003**, *125*, 11291–11298.

Table 5. Crystal Data and Summary of Data Collection and Refinement Details for **4**, **5**, **7** and **10** × **0.5C$_7$H$_8$**

	3	**4**	**7**	**10** × **0.5C$_7$H$_8$**
empirical formula	$C_{33}H_{40}MgN_4Si$	$C_{33}H_{38}MgN_4.C_7H_8$	$C_{30}H_{32}N_4Zn$	$C_{36.50}$ H_{44} N_4 Si Zn
formula weight	545.09	607.12	513.97	632.24
temperature, K	180(2)	180(2)	180(2)	180(2)
wavelength, Å	0.71073	0.71073	0.71073	0.71073
crystal system	triclinic	monoclinic	hexagonal	monoclinic
space group	$P\bar{1}$	$P2_1/c$	$P3_2$	$P2_1/n$
a, Å	9.06(1)	9.152(1)	9.7099(3)	9.715(6)
b, Å	13.58(2)	21.851(3)	9.7099(3)	26.118(2)
c, Å	13.95(2)	17.090(2)	23.409(2)	14.081(9)
α, deg	114.12(2)		90	
β, deg	96.94(3)	95.141(2)	90	104.79(1)
γ, deg	90.90(1)		120	
volume, Å^3	1552(3)	3403.9(8)	1911.4(2)	3454(4)
Z	2	4	3	4
density (calculated), g/cm^3	1.166	1.185	1.340	1.213
absorption coefficient, mm^{-1}	0.123	0.086	0.989	0.775
F(000)	584	1304	810	1334
crystal size, mm^3	0.53 × 0.45 × 0.36	0.81 × 0.75 × 0.68	0.43 × 0.34 × 0.30	0.26 × 0.17 × 0.12
index ranges	$-11 \le h \le 3$	$-7 \le h \le 8$	$-9 \le h \le 9$	$-11 \le h \le 11$
	$-15 \le k \le 15$	$-20 \le k \le 20$	$-9 \le k \le 9$	$-31 \le k \le 31$
	$-5 \le l \le 16$	$-16 \le l \le 16$	$-23 \le l \le 19$	$-16 \le l \le 16$
reflections collected	7900	11188	6887	19976
independent reflections	2085 [*R*(int) = 0.1454]	2936 [*R*(int) = 0.0678]	2588 [*R*(int) = 0.0662]	6077 [*R*(int) = 0.1170]
data/restraints/parameters	2085/0/359	2936/0/414	2588/1/321	6077/48/390
goodness-of-fit on F^2	0.972	1.044	0.829	0.973
Final *R* indices [$I > 2\sigma(I)$]	R_1 = 0.0656	R_1 = 0.0509	R_1 = 0.0467	R1 = 0.0742
	wR_2 = 0.1551	wR_2 = 0.1174	wR_2 = 0.1171	wR2 = 0.1867
R indices (all data)	R_1 = 0.1594	R_1 = 0.0771	R_1 = 0.0596	R1 = 0.1684
	wR_2 = 0.2099	wR_2 = 0.1338	wR_2 = 0.1288	wR2 = 0.2462
largest diff. peak and hole, e Å^{-3}	0.180 and −0.153	0.276 and −0.230	0.424 and −0.281	0.640 and −0.423

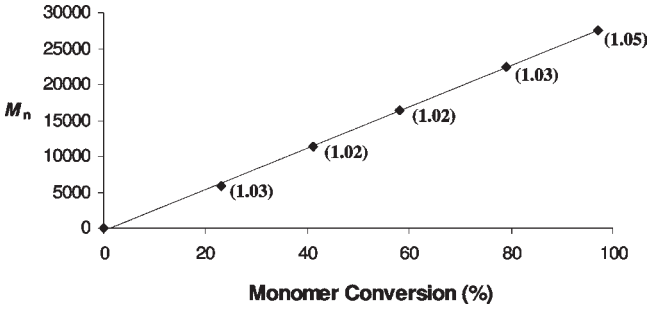

Figure 5. Plot of PLA M_n as a function of monomer conversion (%) for the polymerization of L-LA initiated by **5**; [L-LA]$_0$/[**5**]$_0$ = 200, toluene, 90 °C. (Polydispersity values have been included in parentheses).

optical activity remains almost constant, $[\alpha]_D^{22}$ = 145−148°.

The high level of control afforded by this initiator in the polymerization of L-lactide is further exemplified by the narrow molecular weight distributions and linear correlations between M_n and percentage conversion (Figure 5). These results are characteristic of well-controlled living propagations as well as the existence of a single type of reaction site, a situation similar to the living behavior previously observed in the amidinate-based alkyl magnesium derivatives.[20] As expected, when the polymerization was carried out in THF (entry 6) the activity of **5** dropped and after 5 h only 70% of the monomer was transformed as a result of the competition reaction between THF and the monomer moiety for the metal center. In contrast, when the polymerization was carried out under bulk conditions, 81% of the polymer was recovered after 0.5 h, and the product had a broader polydispersity (M_w/M_n = 1.38, entry 7).

The new hybrid scorpionate/cyclopentadienyl alkyl magnesium derivatives proved to be more active than the analogous amidinate-based alkyl magnesium[20] complexes (entry 8) in the L-LA ROP process, probably as a result of the lower tendency to undergo possible symmetrical (Schlenk)[40] equilibrium competition than the alkyl amidinate-based heteroscorpionate and, therefore, the lower formation of sandwich species versus catalytic performance. In contrast, zinc complexes **10**, **13**, and **14** were found to be much less active than the magnesium derivative **5** (Table 4, entries 9−11), as previously observed for the production of PCL. Thus, after 30 h in toluene at 90 °C, 81% of the monomer was converted in the case of **10**, and the material had a narrow polydispersity index (M_w/M_n = 1.18, entry 9). In contrast, the aliphatic bis(trimethylsilyl)amide derivative **13** did not produce any polymeric materials after 72 h (entry 10) under otherwise identical conditions, as recently reported by our group,[22] when an amidinate-based heteroscorpionate zinc derivative was tested with this aliphatic amide. Notably, the aryloxo zinc derivative **14** showed higher polymerization activity than the alkyl derivative **10** and in 18 h 92% of the monomer was converted with a slightly broader molecular weight distribution (M_w/M_n = 1.19, entry 11).

Initiator **5** was also tested for the polymerization of *rac*-lactide in toluene at 90 °C (Table 4, entries 12−14). Derivative **5** gave 32% conversion of 200 equiv after 4 h (entry 12) and produced a low molecular weight material with a very narrow polydispersity (M_n = 8 800, M_w/M_n = 1.07). Extension of the reaction time to 8 h increased the activity, with conversion rising to 59%, and led to a

(40) (a) Ashby, E. C. *Pure Appl. Chem.* **1980**, *52*, 545–569. (b) Ashby, E. C.; Laemmle, J.; Neumann, H. M. *Acc. Chem. Res.* **1974**, *7*, 272–280. (c) Ashby, E. C. *Quart. Rev., Chem. Soc.* **1967**, 259–285. (d) Kharasch, M. S.; Reinmuth, O. *Grignard Reactions of Nonmetallic Substances*; Prentice-Hall: New York, 1954.

significant increase in the polymer molecular weight and a slight increase in polydispersity (M_n = 15 500, M_w/M_n = 1.12, entry 13). Under bulk conditions 41% of the polymer was recovered after 2 h, and this had a broader polydispersity (M_w/M_n = 1.41, entry 14). We attribute this broad molecular weight distribution to gradual catalyst decomposition on increasing the temperature and a small degree of transesterification and/or slow and incomplete initiation relative to propagation. In all cases (entries 12−14), low melting materials were obtained with the T_m ranging from 126 to 135 °C. As far as we are aware, very few examples of magnesium alkyl initiators[20,21,37a,38,41,42] have been reported to act as active single-site catalysts for the ROP of *rac*-lactide. PLA end-group analysis showed that in all cases (entries 1−7 and 9−14), as for PCL initiated by alkyl magnesium and zinc initiators, the polymerization was initiated by nucleophilic attack of the alkyl group on lactide. Microstructural analysis of the poly(*rac*-lactide) by ^{1}H NMR spectroscopy revealed that **5** exerts a low degree of stereoselectivity. This conclusion is based on the fact that the heterotactic tetrads ***isi*** and ***sis*** were not greatly enhanced as a result of the preference of the consecutive alternate insertion of the L- and D-lactide units into the growing chain. This behavior during the propagation is most probably the result of the low steric demand of the methyl subtituents in the two pyrazole rings. This leads to sterically less congested and more flexible (and therefore less selective) active centers to the incoming lactide, even in the permanent presence of the sterically hindered cyclopentadienyl substituent in the position *cis* to the alkyl leaving group. These results parallel the previous observations reported by Chisholm, Bochmann, and our group on magnesium alkoxides [(BDI)Mg(O^{t}Bu)(THF)][43] and [(η^3-trispyrazolylborate)MgOR],[17d] and magnesium alkyls [(BDI)Mg(η^1-C_3H_5)(THF)][37a] and [Mg(CH_2SiMe_3)(tbpamd)],[20] respectively, which were found to polymerize *rac*-lactide to atactic poly(lactide). However, the results differ from the appreciable preference for the heterotactic poly(lactide) from *rac*-lactide (P_r = 0.68) previously observed in our group[21] on using amidinate-based heteroscorpionate alkyl zinc initiators with the bulky *tert*-butyl substituent in the pyrazole rings.

In conclusion, we report here a facile synthesis of low-coordinative neutral monoalkyl magnesium complexes [Mg(R)(κ^2-η^5-bpzcp)] (**1**−**6**) through the reaction of a series of commercially available Grignard reagents and the lithium salt [Li(bpzcp)(THF)]. Alternatively, hydrolysis of this hybrid lithium salt and subsequent reaction with ZnR_2 cleanly affords the monoalkyl zinc derivatives [Zn(R){κ^2-η^1(π)-bpzcp}] (**7**−**10**) through alkane elimination reactions. Interestingly, single-crystal X-ray diffraction studies on derivatives **4**, **5**, **7**, and **10** reveal that whereas alkyl magnesium derivatives (**1**−**6**) present a η^5 coordination mode for the cyclopentadienyl fragment, zinc derivatives (**7**−**10**) feature a η^1(π) arrangement in the solid state. Furthermore, we have explored the reactivity of this hybrid lithium salt with $ZnCl_2$ to yield a zinc chloride complex [ZnCl{κ^2-η^1(π)-bpzcp}] (**11**) that is an attractive starting material for the successful preparation of the aromatic amide [Zn(NH-4-MeC_6H_4){κ^2-η^1(π)-bpzcp}] (**12**). In contrast, the use of **11** to prepare aliphatic amide derivatives proved fruitless. Alternatively, protonolysis of a zinc and magnesium metal amide/alkyl by the hybrid ligand bpzcpH leads to aliphatic amide and alkoxide complexes [M(R)(bpzcp)] (**13**−**15**).

The alkyl and alkoxide nucleophilicity of the corresponding magnesium and zinc complexes means that they can act as highly effective single-site living initiators for the well-controlled polymerization of polar monomers over a wide range of temperatures. ε-Caprolactone is polymerized within minutes to give high molecular weight polymers with narrow polydispersities. Not surprisingly, the polymerization of LA occurs more slowly than that of CL but offers good control. L-Lactide afforded highly crystalline, isotactic PLA materials with medium molecular weights, polydispersities as narrow as M_w/M_n = 1.02, and very high melting temperatures (T_m = 165 °C). Propagation occurs without observable epimerization with both families of initiators. Polymerization of *rac*-lactide did not result in appreciable levels of selectivity and produced atactic PLA. End group analysis suggests that magnesium and zinc catalysts initiate the polymerization process by alkyl/alkoxide transfer to the monomer. The slow initiation rate and the lack of stereoselectivity in lactide polymerizations have prompted us to reevaluate the ligand design and incorporate groups that are more sterically challenging than the cyclopentadienyl group in an effort to produce high levels of stereocontrol during the propagations.

Experimental Section

General Procedures. All manipulations were performed under nitrogen, using standard Schlenk techniques. Solvents were predried over sodium wire (toluene, *n*-hexane, THF, diethyl ether) or calcium hydride (dichloromethane) and distilled under nitrogen from sodium (toluene), sodium−potassium alloy (*n*-hexane), sodium-benzophenone (THF, diethyl ether), or calcium hydride (dichloromethane). Deuterated solvents were stored over activated 4 Å molecular sieves and degassed by several freeze−thaw cycles. Microanalyses were carried out with a Perkin-Elmer 2400 CHN analyzer. ^{1}H and ^{13}C NMR spectra were recorded on a Varian Mercury FT-400 spectrometer and referenced to the residual deuterated solvent. The NOESY-1D spectra were recorded on a Varian Inova FT-500 spectrometer with the following acquisition parameters: irradiation time 2 s and number of scans 256, using standard VARIANT-FT software. Two-dimensional NMR spectra were acquired using standard VARIANT-FT software and processed using an IPC-Sun computer. $ZnMe_2$, $ZnEt_2$, $ZnCl_2$, ClMgMe, ClMgEt, ClMg^{t}Bu, $MgBu_2$, $ClMgCH_2SiMe_3$, ClMgBz, and 2,4,6-trimethylphenol were purchased from Aldrich. [Mg{N($SiMe_3$)$_2$}$_2$],[44a] [Zn{N($SiMe_3$)$_2$}$_2$],[44b] [Li(CH_2SiMe_3)],[44c] [LiNH-4-MeC_6H_4],[44d] [Li(bpzcp)(THF)][23,24b] and bpzcpH[25] were prepared according to the literature procedures.

(41) Williams, C. K.; Breyfogle, L. E.; Choi, S. K.; Nam, W.; Young, V. G., Jr.; Hillmyer, M. A.; Tolman, W. B. *J. Am. Chem. Soc.* **2003**, *125*, 11350–11359.

(42) Duda, A.; Penczek, S. *Polymers from Renewable Resources: Biopolyesters and Biocatalysts*; Scholz, C., Gross, R. A., Eds.; ACS Symposium Series Vol.764; American Chemical Society: Washington, DC, 2000; p 160.

(43) Chisholm, M. H.; Huffman, J. C.; Phomphrai, K. *J. Chem. Soc., Dalton Trans.* **2001**, 222–224.

(44) (a) Westerhausen, M. *Inorg. Chem.* **1991**, *30*, 96–101. (b) Bürger, H.; Sawodny, W.; Wannagat, U. *J. Organomet. Chem.* **1965**, *3*, 113–120. (c) Hartwell, F. E.; Brown, T. L. *Inorg. Chem.* **1966**, *5*, 1257–1263. (d) Talaleva, T. V.; Kocheschkov, K. A. *Doklady Akademi Nauk SSSR* **1995**, *104*, 260–263.

ε-Caprolactone was dried by stirring over fresh CaH_2 for 48 h, then distilled under reduced pressure and stored over activated 4 Å molecular sieves. L-Lactide and *rac*-lactide were sublimed twice, recrystallized from THF and finally sublimed again prior to use. Gel permeation chromatography (GPC) measurements were performed on a Polymer Laboratories PL-GPC-220 instrument equipped with a TSK-GEL G3000H column and an ELSD-LTII light-scattering detector. The GPC column was eluted with THF at 45 °C at 1 mL/min and was calibrated using eight monodisperse polystyrene standards in the range 580−483000 Da. PLA melting temperatures were measured using a melting point Block SMP 10. The sample was heated up to 100 °C and then heated at a rate of 1 °C/min up to 165 °C. The specific rotation $[\alpha]_D^{22}$ was measured at a concentration of 10 mg/mL in $CHCl_3$ at 22 °C on a Perkin-Elmer 241 Polarimeter equipped with a Na lamp operating at 589 nm with a light path length of 10 cm.

Preparation of Compounds (1−16). Synthesis of [Mg(Me)-(κ^2-η^5-bpzcp)] (1). In a 250 cm^3 Schlenk tube, [Li(bpzcp)(THF)] (1.00 g, 1.95 mmol) was dissolved in dry toluene (70 cm^3) and cooled to −70 °C. A solution of MeMgCl (3.0 M in THF) (0.65 cm^3, 1.95 mmol) was added, and the mixture was allowed to warm up to room temperature and stirred during 1 h. The solvent was evaporated to dryness under reduced pressure to yield a sticky yellow product. The product was washed with hexane and recrystallized from toluene at −26 °C to give compound **1** as yellow crystals. Yield: 0.71 g, 77%. Anal. Calcd for $C_{30}H_{32}MgN_4$: C, 76.19; H, 6.82; N, 11.85. Found: C, 76.29; H, 6.59; N, 11.79. ^{1}H NMR (C_6D_6, 298 K), δ 7.24−6.78 (m, 11 H, CH, Phenyl groups), 6.62 (m, 2H H^d - C_5H_4), 6.06 (m, 2H, H^c - C_5H_4), 5.10 (s, 2H, H^4), 1.99 (s, 6H, Me^3), 1.42 (s, 6H, Me^5), −0.96 (s, 3 H, $MgCH_3$). ^{13}C-{^{1}H} NMR (C_6D_6, 298 K), δ 149.7, 147.6 ($C^{3\ or\ 5}$), 140.8−125.6 (Phenyl groups), 113.9 (C^c - C_5H_4), 109.2 (C^b - C_5H_4), 106.6 (C^d - C_5H_4), 105.3 (C^4), 72.1 (*C*H), 62.4 (C^a), 13.2 (Me^3), 11.1 (Me^5), −10.8 ($MgCH_3$).

Synthesis of [Mg(Et)(κ^2-η^5-bpzcp)] (2). The synthesis of **2** was carried out in an identical manner to **1**. EtMgCl (2.0 M in THF) (0.98 cm^3, 1.95 mmol), [Li(bpzcp)(THF)] (1.00 g, 1.95 mmol). Yield: 0.87 g, 92%. Anal. Calcd for $C_{31}H_{34}MgN_4$: C, 76.46; H, 7.04; N, 11.51. Found: C, 76.61; H, 6.89; N, 11.42. ^{1}H NMR (C_6D_6, 298 K), δ 7.33−6.89 (m, 11H, CH, Phenyl groups), 6.76 (m, 2H H^d -C_5H_4), 6.12 (m, 2H H^c-C_5H_4), 5.20 (s, 2 H, H^4), 2.11 (s, 6H, Me^3), 1.92 (t, 3H, $^3J_{H-H}$ = 8.4 Hz, $MgCH_2C\mathit{H_3}$), 1.50 (s, 6H, Me^5), −0.09 (q, 2 H, $^3J_{H-H}$ = 8.4 Hz, $Mg\underline{CH_2}CH_3$). ^{13}C-{^{1}H} NMR (C_6D_6, 298 K), δ 149.6, 147.6 ($C^{3\ or\ 5}$), 140.8−128.5 (Phenyl groups), 113.9 (C^c - C_5H_4), 108.9 (C^b - C_5H_4), 106.5 (C^d - C_5H_4), 104.8 (C^4), 72.1 (*C*H), 62.5 (C^a), 13.8 ($MgCH_2\underline{CH_3}$), 12.9 (Me^3), 11.0 (Me^5), 1.44 ($Mg\underline{CH_2}CH_3$).

Synthesis of [Mg(^{n}Bu)(κ^2-η^5-bpzcp)] (3). In a 250 cm^3 Schlenk tube, bpzcpH (1.00 g, 2.30 mmol) was dissolved in dry toluene (70 cm^3) and cooled to −70 °C. A solution of $MgBu_2$ (1.0 M in heptane) (2.30 cm^3, 2.30 mmol) was added, and the mixture was allowed to warm up to room temperature and stirred during 16 h. The solvent was evaporated to dryness under reduced pressure to yield a sticky yellow product. The product was washed with hexane and recrystallized from toluene at −26 °C to give compound **3** as yellow crystals. Yield: 0.94 g, 88%. Anal. Calcd for $C_{33}H_{38}MgN_4$: C, 76.96; H, 7.44, N, 10.88. Found: C, 76.91; H, 7.29; N, 10.71. ^{1}H NMR (C_6D_6, 298 K), δ 7.32−6.87 (m, 11H, CH, Phenyl groups), 6.74 (m, 2H, H^d - C_5H_4), 6.12 (m, 2H, H^c- C_5H_4), 5.20 (s, 2H, H^4), 2.11 (s, 6H, Me^3), 1.89 (m, 4H, $MgCH_2C\mathit{H_2}C\mathit{H_2}CH_3$), 1.49 (s, 6H, Me^5), 1.34 (t, 3H, $^3J_{H-H}$ = 7.6 Hz, $\underline{MgCH_2CH_2CH_2C\mathit{H_3}}$), −0.09 (m, 2 H, $^3J_{H-H}$ = 6.0 Hz, $Mg\underline{C\mathit{H_2}CH_2CH_2CH_3}$). ^{13}C-{^{1}H} NMR ($C_6D_6$, 298 K), δ 149.6, 147.6 ($C^{3\ or\ 5}$), 140.7−118.5 (Phenyl groups), 113.7 (C^c - C_5H_4), 108.9 (C^b - C_5H_4), 106.5 (C^d - C_5H_4), 104.9 (C^4), 72.0 (*C*H), 62.4 (C^a), 33.2, 32.6 ($MgCH_2\underline{CH_2}\mathit{CH_2}CH_3$), 14.6 ($MgCH_2CH_2CH_2\underline{CH_3}$), 12.9 ($Me^3$), 11.2 ($\underline{MgCH_2}CH_2CH_2CH_3$), 10.9 ($Me^5$).

Synthesis of [Mg(^{t}Bu)(κ^2-η^5-bpzcp)] (4). The synthesis of **4** was carried out in an identical manner to **1**. ^{t}BuMgCl (1.0 M in THF) (1.95 cm^3, 1.95 mmol), [Li(bpzcp)(THF)] (1.00 g, 1.95 mmol). Yield: 0.89 g, 89%. Anal. Calcd for $C_{33}H_{38}MgN_4$: C, 76.96; H, 7.44; N, 10.88. Found: C, 77.09; H, 7.57; N, 10.65. ^{1}H NMR (C_6D_6, 298 K), δ 7.23−6.86 (m, 11H, CH, Phenyl groups), 6.76 (m, 2H, H^d - C_5H_4), 5.98 (m, 2H, H^c - C_5H_4), 5.22 (s, 2H, H^4), 2.12 (s, 6 H, Me^3), 1.51 (s, 9H, Mg^{t}Bu), 1.46 (s, 6H, Me^5). ^{13}C-{^{1}H} NMR (C_6D_6, 298 K), δ 149.8, 147.5 ($C^{3\ or\ 5}$), 141.2−128.4 (Phenyl groups), 112.6 (C^c - C_5H_4), 108.2 (C^b - C_5H_4), 106.8 (C^d - C_5H_4), 105.3 (C^4), 72.1 (*C*H), 62.5 (C^a), 35.1 ($Mg\underline{C}(CH_3)_3$), 21.7 ($MgC(\underline{CH_3})_3$), 13.8 (Me^3), 11.0 (Me^5).

Synthesis of [Mg(CH_2SiMe_3)(κ^2-η^5-bpzcp)] (5). The synthesis of **5** was carried out in an identical manner to **1**. Me_3SiCH_2MgCl (1.0 M in Et_2O) (1.95 cm^3, 1.95 mmol), [Li(bpzcp)(THF)] (1.00 g, 1.95 mmol). Yield: 0.94 g, 88%. Anal. Calcd for $C_{33}H_{40}MgN_4Si$: C, 72.71; H, 7.40; N, 10.28. Found: C, 72.91; H, 7.77; N, 10.51. ^{1}H NMR (C_6D_6, 298 K), δ 7.29−6.86 (m, 11H, CH, Phenyl groups), 6.74 (m, 2H, H^d - C_5H_4), 6.10 (m, 2H, H^c - C_5H_4), 5.18 (s, 2H, H^4), 2.09 (s, 6 H, Me^3), 1.45 (s, 6H, Me^5), 0.59 (s, 9H, $MgCH_2Si\mathit{Me_3}$), −1.31 (s, 2H, $Mg\underline{C\mathit{H_2}}SiMe_3$). ^{13}C-{^{1}H} NMR ($C_6D_6$, 298 K), δ 149.7, 147.5 ($C^{3\ or\ 5}$), 140.9−126.5 (Phenyl groups), 113.9 (C^c - C_5H_4), 109.2 (C^b - C_5H_4), 106.5 (C^d - C_5H_4), 105.8 (C^4), 72.1 (*C*H), 62.3 (C^a), 13.8 (Me^3), 11.0 (Me^5), 5.15 ($MgCH_2Si\mathit{Me_3}$), −4.24 ($Mg\underline{CH_2}SiMe_3$).

Synthesis of [Mg(Bz)(κ^2-η^5-bpzcp)] (6). The synthesis of **6** was carried out in an identical manner to **1**. BzMgCl (2.0 M in THF) (0.975 cm^3, 1.95 mmol), [Li(bpzcp)(THF)] (1.00 g, 1.95 mmol). Yield: 0.87 g, 81%. Anal. Calcd for $C_{36}H_{36}MgN_4$: C, 78.76; H, 6.61; N, 10.21. Found: C, 78.69; H, 6.57; N, 10.33. ^{1}H NMR (C_6D_6, 298 K), δ 7.38−6.86 (m, 16H, CH, Phenyl groups), 6.64 (m, 2H, H^d - C_5H_4), 6.00 (m, 2H, H^c - C_5H_4), 5.15 (s, 2H, H^4), 1.99 (s, 6H, Me^3), 1.44 (s, 6H, Me^5), 0.29 (s, 2H, $Mg\underline{CH_2}C_6H_5$). ^{13}C-{^{1}H} NMR (C_6D_6, 298 K), δ 149.9, 147.3 ($C^{3\ or\ 5}$), 141.1−127.8 (Phenyl groups), 114.2 (C^c - C_5H_4), 108.6 (C^b - C_5H_4), 106.7 (C^d - C_5H_4), 104.9 (C^4), 72.1 (*C*H), 62.5 (C^a), 13.5 (Me^3), 11.0 (Me^5) 1.35 ($Mg\underline{CH_2}C_6H_5$).

Synthesis of [Zn(Me){κ^2-η^1(π)-bpzcp}] (7). In a 250 cm^3 Schlenk tube, bpzcpH (1.00 g, 2.30 mmol) was dissolved in dry toluene (70 cm^3) and cooled to −70 °C. A solution of $ZnMe_2$ (2.0 M in toluene) (1.15 cm^3, 2.30 mmol) was added, and the mixture was allowed to warm up to room temperature and stirred during 16 h. The solvent was evaporated to dryness under reduced pressure to yield a sticky yellow product. The product was washed with hexane and recrystallized from toluene at −26 °C to give compound **7** as yellow crystals. Yield: 0.97 g, 82%. Anal. Calcd for $C_{30}H_{32}N_4Zn$: C, 70.10; H, 6.28; N, 10.90. Found: C, 69.98; H, 6.44; N, 10.79. ^{1}H NMR (C_6D_6, 298 K), δ 7.14−6.90 (m, 10H, Phenyl groups), 6.95 (m, 2H, H^d - C_5H_4) 6.79 (s, 1H, CH), 6.16 (m, 2H, H^c - C_5H_4), 5.18 (s, 2H, H^4), 1.97 (s, 6 H, Me^3), 1.58 (s, 6H, Me^5), −0.20 (s, 3 H, $ZnCH_3$). ^{13}C-{^{1}H} NMR (C_6D_6, 298 K), δ 149.9, 146.9 ($C^{3\ or\ 5}$), 140.8−126.6 (Phenyl groups), 117.6 (C^b - C_5H_4), 115.4 (C^c - C_5H_4), 108.0 (C^d - C_5H_4), 106.3 (C^4), 70.8 (*C*H), 63.5 (*C*Ph_2), 13.0 (Me^3), 11.3 (Me^5), −12.9 ($ZnCH_3$).

Synthesis of [Zn(Et){κ^2-η^1(π)-bpzcp}] (8). The synthesis of **8** was carried out in an identical manner to **7**. $ZnEt_2$ (1.0 M in hexane) (2.30 cm^3, 2.30 mmol), bpzcpH (1.00 g, 2.30 mmol). Yield: 1.04 g, 86%. Anal. Calcd for $C_{31}H_{34}N_4Zn$: C, 70.51; H, 6.49; N, 10.61. Found: C, 70.27; H, 6.33; N, 10.34. ^{1}H NMR (C_6D_6, 298 K), δ 7.13−6.91 (m, 10H, Phenyl groups), 7.02 (m, 2H, H^d - C_5H_4), 6.80 (s, 1H, CH), 6.14 (m, 2H, H^c - C_5H_4), 5.20 (s, 1H, H^4), 1.99 (s, 6H, Me^3), 1.76 (t, 3H, $^3J_{H-H}$ = 6.8 Hz, $ZnCH_2C\mathit{H_3}$), 1.58 (s, 6H, Me^5), −0.61 (q, 2H, $^3J_{H-H}$ = 6.8 Hz, $Zn\underline{C\mathit{H_2}}CH_3$). ^{13}C-{^{1}H} NMR ($C_6D_6$, 298 K), δ 149.7, 146.9 ($C^{3\ or\ 5}$), 140.8−127.3 (Phenyl groups), 117.6 (C^b - C_5H_4), 114.4 (C^c - C_5H_4), 107.8 (C^d - C_5H_4), 106.2 (C^4), 70.8 (*C*H), 63.5 (*C*Ph_2), 13.7 ($ZnCH_2\underline{CH_3}$), 12.9 (Me^3), 11.2 (Me^5), 0.4 ($Zn\underline{CH_2}CH_3$).

Synthesis of [Zn(^{t}Bu){κ^2-η^1(π)-bpzcp}] (9). Compound **9** was made by a one-pot reaction. In a 250 cm^3 Schlenk tube, $ZnCl_2$

(0.45 g, 3.30 mmol) was dissolved in dry diethyl ether (70 cm^3) and cooled to −70 °C. A solution of ^tBuLi (1.7 M in pentane) (3.88 cm^3, 6.60 mmol) was added, and the mixture was allowed to warm up to room temperature and stirred for 1 h. An increasing turbidity developed, and this finally led to the formation of a white suspension. The suspension was filtered, and the filtrate corresponding to Zn^tBu_2 was added to a precooled (−20 °C) solution of bpzcpH (1.43 g, 3.30 mmol) in diethyl ether. The mixture was stirred at this temperature for 16 h. The volatiles were removed, and the resulting sticky yellow solid was washed with hexane (30 cm^3) and recrystallized from toluene to give the title compound **9** as yellow crystals. Yield: 1.45 g, 79%. Anal. Calcd for $C_{33}H_{38}N_4Zn$: C, 71.28; H, 6.89; N, 10.08. Found: C, 70.99; H, 6.57; N, 10.22. ^1H NMR (C_6D_6, 298 K), δ 7.13−6.83 (m, 10 H, Phenyl groups), 6.92 (m, 2H, H^d - C_5H_4), 6.67 (s, 1H, CH), 6.26 (m, 2H, H^c- C_5H_4), 5.20 (s, 2H, H^4), 2.11 (s, 6H, Me^3), 1.57 (s, 9H, Zn^tBu), 1.50 (s, 6H, Me^5). ^{13}C-{^1H} NMR (C_6D_6, 298 K), δ 149.3, 146.7 ($C^{3\ or\ 5}$), 141.3−126.2 (Phenyl groups), 117.1 (C^b - C_5H_4), 115.5 (C^c - C_5H_4), 109.9 (C^d - C_5H_4), 106.7 (C^4), 70.8 (*C*H), 65.2 (*C*Ph_2), 34.6 (ZnC(*C*H_3)$_3$), 32.1 (Zn*C*$(CH_3)_3$), 14.0 (Me^3), 11.3 (Me^5).

Synthesis of [Zn(CH_2SiMe_3){κ^2-η^1(π)-bpzcp}] × 0.5 C_7H_8 (10). Compound **10** was made by a one-pot reaction. A solution of [Li(CH_2SiMe_3)] (0.62 g, 6.60 mmol) in diethyl ether was added to a cooled (−40 °C), stirred solution of $ZnCl_2$ (0.45 g, 3.30 mmol) in diethyl ether in a 250 mL Schlenk tube. The mixture was allowed to warm up to room temperature and stirred for 1 h. An increasing turbidity developed, and this finally led to the formation of a white suspension. The suspension was filtered, and the filtrate corresponding to Zn(CH_2SiMe_3)$_2$ was added to a precooled (−20 °C) solution of bpzcpH (1.43 g, 3.30 mmol) in diethyl ether. The mixture was stirred at this temperature for 16 h. The volatiles were removed, and the sticky yellow solid obtained was washed with hexane (30 cm^3) and recrystallized from toluene to give the title compound **10** as yellow crystals. Yield: 1.61 g, 77%. Anal. Calcd for $C_{33}H_{40}N_4SiZn \times 0.5\ C_7H_8$ C, 69.35; H, 6.96; N, 8.86. Found: C, 69.53; H, 6.89; N, 8.91. ^1H NMR (C_6D_6, 298 K), δ 7.13−6.88 (m, 10H, Phenyl groups), 6.95 (m, 2H, H^d - C_5H_4), 6.78 (s, 1H, CH), 6.09 (m, 2 H, H^c- C_5H_4), 5.19 (s, 2H, H^4), 2.08 (s, 6H, Me^3), 1.56 (s, 6H, Me^5), 0.51 (ZnCH_2Si*Me*$_3$), −0.57 (ZnC*H*$_2$SiMe_3). ^{13}C-{^1H} NMR (C_6D_6, 298 K), δ 149.9, 146.9 ($C^{3\ or\ 5}$), 140.8−126.6 (Phenyl groups), 117.6 (C^b - C_5H_4), 116.4 (C^c - C_5H_4), 107.5 (C^d - C_5H_4), 106.2 (C^4), 70.8 (*C*H), 63.6 (*C*Ph_2), 13.7 (Me^3), 11.4 (Me^5), 3.96 (ZnCH_2Si*Me*$_3$), −6.4 (Zn*C*H_2SiMe_3).

Conversion from [Mg(R)(κ^2-η^5-bpzcp)] (1, 2, 4, and 5) into [Zn(R){κ^2-η^1(π)-bpzcp}] (7−10). As an example, in a 250 cm^3 Schlenk tube, [Mg(CH_2SiMe_3){κ^2-η^5-bpzcp}] (**5**) (1.00 g, 1.83 mmol) was dissolved in dry toluene (60 cm^3) and reacted with an ether (20 cm^3) solution of $ZnCl_2$ (0.25 g, 1.83 mmol). The mixture was stirred during 24 h. The solvent was evaporated to dryness under reduced pressure, and the product was extracted and recrystallized from toluene to give compound (**10**) as white crystals. Yield: 0.925 g, 86%.

Synthesis of [ZnCl{κ^2-η^1(π)-bpzcp}] (11). In a 250 cm^3 Schlenk tube, [Li(bpzcp)(THF)] (1.17 g, 2.30 mmol) was dissolved in dry THF (70 cm^3) and cooled to −70 °C. A solution of $ZnCl_2$ (0.31, 2.30 mmol) was added, and the mixture was allowed to warm up to room temperature and stirred during 16 h. The solvent was evaporated to dryness under reduced pressure, and the product was extracted and recrystallized from CH_2Cl_2 to give compound **11** as white crystals. Yield: 0.92 g, 75%. Anal. Calcd for $C_{29}H_{29}ClN_4Zn$: C, 65.17; H, 5.47; N, 10.48. Found: C, 65.38; H, 5.34; N, 10.11. ^1H NMR ($CDCl_3$, 298 K), δ 7.25−7.12 (m, 11H, Phenyl groups, CH), 6.48 (m, 2H, H^d - C_5H_4), 5.53 (m, 2H, H^c - C_5H_4), 5.84 (s, 2H, H^4), 2.29 (s, 6 H, Me^3), 2.28 (s, 6H, Me^5). ^{13}C-{^1H} NMR ($CDCl_3$, 298 K), δ 151.8, 145.9 ($C^{3\ or\ 5}$), 141.6−126.6 (Phenyl groups), 115.7 (C^c - C_5H_4), 112.6 (C^b - C_5H_4), 107.0 (C^d - C_5H_4), 101.5 (C^4), 72.0 (*C*H), 65.4 (C^a), 13.5 (Me^3), 12.1 (Me^5).

Synthesis of [Zn(NH-4-MeC_6H_4){κ^2-η^1(π)-bpzcp}] (NH-4-MeC_6H_4 = *p*-toluidine) (12). In a 250 cm^3 Schlenk tube, compound **11** (0.92 g, 1.72 mmol) was dissolved in dry THF (70 cm^3) and cooled to −70 °C. LiNHAr (NHAr = *para*-toluidine) (0.19 g, 1.72 mmol) was dissolved in THF (30 cm^3) and added dropwise to the solution. The mixture was allowed to warm up and stirred at room temperature during 1 h. The solvent was evaporated to dryness under reduced pressure to yield a sticky yellow product. The product was extracted from toluene and recrystallized at −26 °C to give compound **12** as yellow crystals. Yield: 0.71 g, 68%. Anal. Calcd for $C_{36}H_{37}N_5Zn$: C, 71.45; H, 6.16; N, 11.57. Found: C, 71.10; H, 6.46; N, 11.91. ^1H NMR (Toluene-d_8, 298 K), δ 7.15−7.01 (m, 11H, CH, Phenyl groups), 6.92 (m, 2H, H^d - C_5H_4), 6.78, 6.69 (2 m, 2H each, H − HN*C*$_6$*H*$_4$Me), 5.77 (m, 2H, H^c - C_5H_4), 5.18 (s, 2H, H^4), 3.22 (s, 1H, *H*N*C*$_6$H$_4$Me), 2.13 (s, 3H, HN*C*$_6$H$_4$*Me*), 1.95 (s, 6 H, Me^3), 1.55 (s, 6H, Me^5), ^{13}C-{^1H} NMR (Toluene-d_8, 298 K), δ 149.8, 146.7 ($C^{3\ or\ 5}$), 140.9−126.5 (Phenyl groups, HN*C*$_6$H$_4$Me), 117.6 (C^b - C_5H_4), 114.7 (C^c - C_5H_4), 108.2 (C^d - C_5H_4), 106.3 (C^4), 70.8 (*C*H), 63.5 (*C*Ph_2), 25.4 (HNC_6H_4*Me*), 13.1 (Me^3), 11.4 (Me^5).

Synthesis of [Zn{$N(SiMe_3)_2$}{κ^2-η^1(π)-bpzcp}] (13). In a 250 cm^3 Schlenk tube, Zn[$N(SiMe_3)_2$]$_2$ (0.88, 2.30 mmol) was dissolved in dry toluene (70 cm^3) and cooled to −70 °C. A solution of bpzcpH (1.00 g, 2.30 mmol) in toluene (30 cm^3) was added, and the mixture was allowed to warm up to room temperature and stirred during 4 h. The solvent was evaporated to dryness under reduced pressure to yield a sticky yellow product. The product was washed with hexane and recrystallized from toluene at −26 °C to give compound **13** as white crystals. Yield: 1.14 g, 74%. Anal. Calcd for $C_{35}H_{47}N_5Si_2Zn$: C, 63.75; H, 7.18; N, 10.62. Found: C, 63.45; H, 7.23; N. 10.75. ^1H NMR (Toluene-d_8, 298 K), δ 7.28−6.87 (m, 11H, CH, Phenyl groups), 6.83 (m, 2H, H^d - C_5H_4), 5.70 (m, 2H, H^c - C_5H_4), 5.36 (s, 2H, H^4), 2.22 (s, 6H, Me^3), 1.88 (s, 6H, Me^5), 0.15 (s, 18H, ZnN(*SiMe*$_3$)$_2$). ^{13}C-{^1H} NMR (Toluene-d_8, 278 K), δ 151.3, 147.2 ($C^{3\ or\ 5}$), 141.3−126.2 (Phenyl groups), 125.5 (C^c - C_5H_4), 117.74 (C^d - C_5H_4), 106.5 (C^4), 106.0 (C^b - C_5H_4), 71.2 (*C*H), 64.8 (C^a), 13.9 (Me^3), 11.4 (Me^5), 2.5 (ZnN(*SiMe*$_3$)$_2$).

Synthesis of [Zn(2,4,6-$Me_3C_6H_2O$){κ^2-η^1(π)-bpzcp}] (2,4,6-$Me_3C_6H_2O$ = mesityloxy) (14). Compound **14** was prepared in a one-pot reaction. A solution of 2,4,6-trimethylphenol (0.31 g, 2.30 mmol) in THF (30 cm^3) was added to a cooled (−40 °C), stirred solution of $ZnEt_2$ (0.28 g, 2.30 mmol) in THF (30 cm^3) in a 250 mL Schlenk tube. The mixture was allowed to warm up to room temperature and stirred for 1 h at room temperature. A solution of bpzcpH (1.00 g, 2.30 mmol) in THF (30 cm^3) was added, and the mixture was heated to 50 °C over 2 h. The volatiles were removed, and the resulting sticky white solid was washed with hexane (60 cm^3) and recrystallized from toluene to give the title compound **14** as white crystals. Yield: 1.30 g, 89%. Anal. Calcd for $C_{38}H_{40}N_4OZn$: C, 71.97; H, 6.36; N, 8.83. Found: C, 72.11; H, 6.61; N, 8.72. ^1H NMR ($CDCl_3$, 298 K), δ 7.23−7.00 (m, 11H, CH, Phenyl groups), 6.66 (s, 2H, $H^{3,5}$ - OR), 6.48 (m, 2H, H^d - C_5H_4), 5.81 (s, 2H, H^4), 5.56 (m, 2H, H^c- C_5H_4), 2.20 (s, 6H, Me^3), 2.15 (s, 3H, Me^4 − OR), 2.03 (s, 6H, Me^5), 1.93 (s, 6H, $Me^{2,6}$ − OR). ^{13}C-{^1H} NMR ($CDCl_3$, 298 K), δ 151.9 (C^b − OR), 146.3, 141.8 ($C^{3\ or\ 5}$), 129.6−126.5 (Phenyl groups, Zn−O-*C*$_6$*H*$_3$(Me)$_3$), 122.3 (C^b - C_5H_4), 115.4 (C^c - C_5H_4), 106.9 (C^d - C_5H_4), 102.0 (C^4), 72.3 (*C*H), 62.2 (*C*Ph_2), 20.7 (Me^4 − OR), 18.4 ($Me^{2,6}$ − OR), 13.2 (Me^3), 12.4 (Me^5).

Synthesis of [Mg{$N(SiMe_3)_2$}(κ^2-η^5-bpzcp)] (15). In a 250 cm^3 Schlenk tube, [Mg{$N(SiMe_3)_2$}$_2$]$_2$ (0.79, 2.30 mmol) was dissolved in dry toluene (70 cm^3) and cooled to −70 °C. A solution of bpzcpH (2.00 g, 4.60 mmol) in toluene (30 cm^3) was added dropwise, the mixture allowed to warm up to room temperature and stirred during 16 h. The solvent was evaporated to dryness under reduced pressure to yield a sticky yellow product.

The product was recrystallized from toluene at −26 °C to give compound **15** as white crystals. Yield: 2.15 g, 81%. Anal. Calcd for $C_{35}H_{47}N_5Si_2Mg$: C, 67.99; H, 7.66; N, 11.33. Found: C, 67.71; H, 7.33; N. 11.15. ^{1}H NMR (Toluene-d_8, 298 K), δ 7.32−6.86 (m, 11H, CH, Phenyl groups), 6.61 (m, 2H, H^d - C_5H_4), 5.93 (m, 2H, H^c - C_5H_4), 5.32 (s, 2H, H^4), 2.28 (s, 6H, Me^3), 1.60 (s, 6H, Me^5), 0.08 (s, 18H, $MgN(\underline{SiMe_3})_2$). ^{13}C-{^{1}H} NMR (Toluene-d_8, 328 K), δ 151.3, 147.2 ($C^{3\ or\ 5}$), 141.1−126.42 (Phenyl groups), 125.3 (C^c - C_5H_4), 116.13 (C^d - C_5H_4), 106.2 (C^4), 105.7 (C^b - C_5H_4), 71.2 (*C*H), 64.7 (C^a), 14.1 (Me^3), 11.3 (Me^5), 2.7 ($MgN(\underline{SiMe_3})_2$).

X-ray Crystallographic Structure Determination for Complexes 4, 5, 7, and 10 × 0.5C$_7$H$_8$. A summary of crystal data collection and refinement parameters for all compounds is given in Table 5.

Single crystals of **4**, **5**, **7**, and **10** × **0.5C$_7$H$_8$** were mounted on a glass fiber and transferred to a Bruker X8 APEX II CCD-based diffractometer equipped with a graphite monochromated Mo−Kα radiation source (λ = 0.71073 Å). Data were integrated using SAINT,[45] and an absorption correction was performed with the program SADABS.[46] The software package SHELXTL version 6.12[47] was used for space group determination, and structure solution and refinement were carried out by full-matrix least-squares methods based on F^2. All non-hydrogen atoms were refined with anisotropic thermal parameters. Hydrogen atoms were placed using a "riding model" and included in the refinement at calculated positions. The complex **10** × **0.5C$_7$H$_8$** crystallizes with half a molecule of toluene in the asymmetric unit. The toluene solvent is highly disordered about an inversion center and was refined with soft restraints and constraints, and their carbon atoms were refined with isotropic displacement parameters.

Polimerization Procedures

Polymerizations of ε-caprolactone (CL) were carried out on a Schlenk line in a flame-dried round-bottomed flask equipped with a magnetic stirrer. In a typical procedure, the initiator was dissolved in the appropriate amount of solvent and temperature equilibration was ensured by stirring the solution for 15 min in a temperature-controlled bath. ε-CL was injected and polymerization times were measured from that point. Polymerizations were terminated by addition of acetic acid (5 vol-%) in methanol. Polymers were precipitated in methanol, filtered, dissolved in THF, reprecipitated in methanol, and dried in vacuo to constant weight.

Polymerizations of L-lactide and *rac*-lactide (LA) were performed on a Schlenk line in a flame-dried round-bottomed flask equipped with a magnetic stirrer. The Schlenk tubes were charged in the glovebox with the required amount of *rac*-lactide and initiator, separately, and then attached to the vacuum line. The initiator and monomer were dissolved in the appropriate amount of solvent, and temperature equilibration was ensured in both Schlenk flasks by stirring the solutions for 15 min in a bath. The appropriate amount of initiator was added by syringe, and polymerization times were measured from that point. Polymerizations were stopped by injecting a solution of acetic acid (5 vol-%) in methanol. Polymers were precipitated in methanol, filtered, dissolved in THF, reprecipitated in methanol, and dried in vacuo to constant weight.

Acknowledgment. We gratefully acknowledge financial support from the Ministerio de Educación y Ciencia (Dirección General de Investigación), Spain (Grants CTQ2008-05892/BQU, CTQ2008-00318/BQU, Consolider-Ingenio 2010 ORFEO CSD2007-00006), Consejería de Educación, Comunidad de Madrid, Spain (Grant S-0505/PPQ/0328) and Consejería de Educación y Ciencia, Comunidad de Castilla-La Mancha, Spain (Grant PCI08-0010).

Supporting Information Available: Full crystallographic data for **4**, **5**, **7**, and **10**. This material is available free of charge via the Internet at http://pubs.acs.org.

(45) *SAINT+ v7.12a, Area-Detector Integration Program*; Bruker-Nonius AXS: Madison, WI, 2004.

(46) Sheldrick, G. M. *SADABS version 2004/1, A Program for Empirical Absorption Correction*; University of Göttingen: Göttingen, Germany, 2004.

(47) *SHELXTL-NT version 6.12, Structure Determination Package*; Bruker-Nonius AXS: Madison, WI, 2001.

(48) Barakat, I.; Dubois, Ph.; Jérôme, R.; Teyssié, Ph. *J. Polym. Sci., Part A: Polym. Chem.* **1993**, *31*, 505–514.